NTNU – Trondheim
Norwegian University of
Science and Technology

Paleobathymetric reconstruction in the Hammerfest and Tromsø basins, southwestern Barents Sea

Susanne Heinicke

Petroleum Geosciences
Submission date: June 2012
Supervisor: Stephen John Lippard, IGB
Co-supervisor: Matthias Daszinnies, SINTEF Petroleum Research

Norwegian University of Science and Technology
Department of Geology and Mineral Resources Engineering

Acknowledgements

This master thesis was accomplished in the period from January until June in 2012 at SINTEF Petroleum Research.

I would like to express my gratitude to my supervisor Matthias Christian Daszinnies for all his great support and advice during the project. Many thanks also to my supervisor at NTNU, Prof. Stephen Lippard.

Especially, a thanks goes to AGR (Oslo) for providing the seismic and well data for this study. I would also like to thank Etor Querendez for his support with the depth conversion of the seismic data.

Thanks as well to the employees at the Basin Modelling Department, SINTEF Petroleum Research for their kindness and helpfulness.

Abstract

Seismic interpretation of 13 lines has been conducted in the Hammerfest and Tromsø basin areas in the southwestern Barents Sea. Based on interpretations, a 3D Geomodel comprising 10 layers has been constructed. Depth conversion of the Geomodel was accomplished after building of the herein required velocity model.

Paleobathymetric reconstruction was performed for 9 time intervals from Top Oxfordian/Late Jurassic until Intra Sotbakken/Base Pliocene utilizing SINTEF´s basin modeling tool SEMI Paleowater. The restoration method is based on the information about depositional geometries from seismic sequences combined with zero or near zero water depth indicators. The time intervals have been restored using the deep marine infill scenario.

The reconstruction showed that the Early Cretaceous paleo-water depth was greatly influenced by the Late Jurassic-Early Cretaceous rifting episode that resulted in the formation of deep marine basins and structural highs. Differential subsidence during the Cretaceous led to more stable areas in the east and rapidly subsiding basins in the west of the study area. Compressional tectonics in the Early Paleogene resulted in the development of the Senja Ridge as a positive structure. From the Oligocene until the Miocene, a period of shallow marine conditions was restored in the Hammerfest and Tromsø basins. The transition to a passive continental margin and resulting thermal subsidence led to a new deepening in the Neogene.

Table of Contents

Table of Figures

Table of Tables

1. Introduction

Exploration for hydrocarbons started in the Barents Sea in 1980s and the area is about to become a place for future exploration in Norway. Periods of uplift and erosion have had a large effect on the generation and accumulation of hydrocarbons (Ohm *et al.,* 2008). Associated paleobathymetry variations in time are also an important parameter in basin analysis. Paleo-water depth can have a major influence on the geometries of the horizons reconstructed in the decompaction modeling process. Thus it influences the burial history modeling and the calculated hydrocarbon migration pathways. However, paleobathymetry has often been neglected in basin modeling studies (Kjennerud & Sylta, 2001).

Two approaches are most common to estimate paleobathymetry. These are based on 1) local well data e.g. micropaleontological, sedimentological or geochemical data and 2) regional based data like seismic profiles (e.g. Kjennerud, 2001). In order to provide quantitative paleobathymetric estimates it is often necessary to combine both approaches.

Kjennerud (2001) presented a method for restoring geological profiles using depositional geometries and zero water depth indications as the main constraints. Based on that, a 3D approach for paleo-water depth reconstruction was implemented in SINTEF´s hydrocarbon migration software SEMI.

The area of interest of this study is in the southwestern Barents Sea, specifically the area around the Hammerfest and Tromsø basins. This area consists of deep sedimentary rift basins and characteristic positive structures e.g. the Loppa High.

Extensional tectonics in the Barents Sea have occurred already in Carboniferous and Permian times. However, the western Barents shelf has been most tectonically active during Mesozoic and Cenozoic times. Two main phases are observed: Middle - Late Jurassic and Early Cretaceous rifting and basin formation and Early Cenozoic rifting and opening of the Norwegian – Greenland Sea (Faleide *et al.,* 1993, Gudlaugsson *et al*., 1998).

The aim of this study is the paleo-water depth reconstruction from Late Jurassic/Base Hekkingen (Top Oxfordian) to Intra Sotbakken/Base Pliocene in the southwestern Barents Sea. In total 9 time steps will be reconstructed using SINTEF´s software SEMI Paleowater. Prior to the reconstruction 10 depth maps have been generated as an input for the paleo-water restoration. This was accomplished by interpretation of 2D seismic data and the construction of a Geomodel in PETREL. The results of the paleobathymtric reconstruction will be compared to the earlier completed Integrated Barents Sea Study – Basin Modelling Upgrade from 2008 (IBS-BMU 2008, Inthorn *et al., 2008*).

2. Geological Setting

2.1 Regional setting of the Barents Sea

The Barents Sea is a wide epicontinental sea in the area north of Norway and Russia (Fig. 1). It developed due to the opening of the North Atlantic and Arctic oceans in response to the break up between Greenland and Norway in the Late Paleocene (Dengo & Røssland, 1992). In the north, the Barents Sea is bordered by the Svalbard archipelago and Franz-Josef Land and towards the east by the extension of the Ural mountain chain through Novaya Zemlya. The Kola Peninsula and the coast of northern Norway define the southern border and the deeper waters in the Norwegian Sea mark the western limit (Henriksen *et al*., 2011).

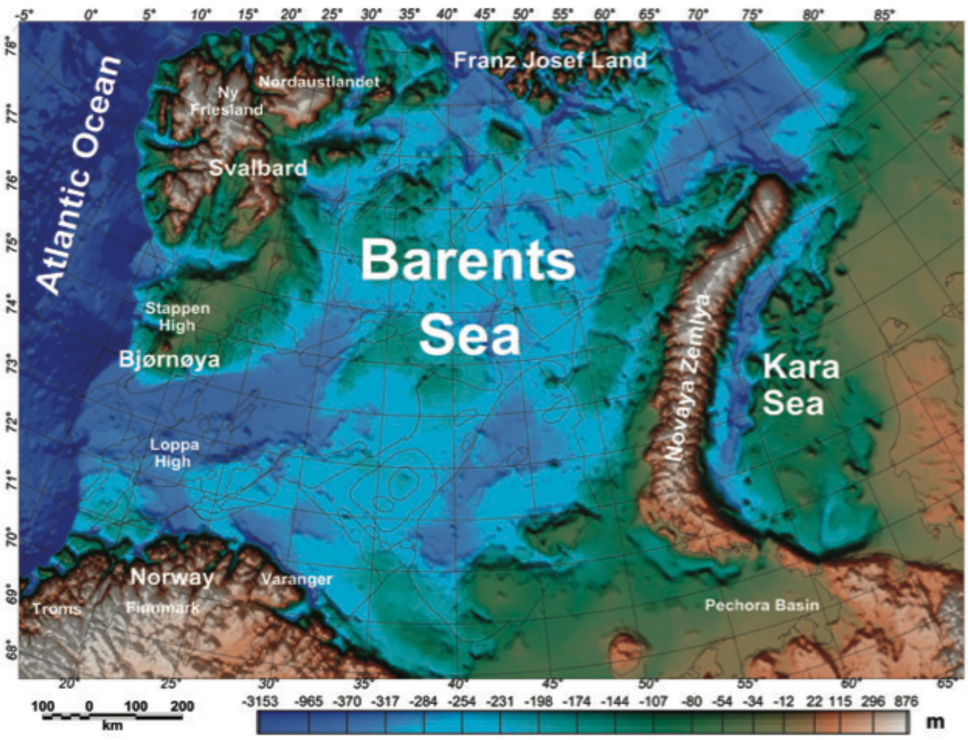

Figure 1. Bathymetric and topographic map of the Barents Sea Shelf and surrounding landmasses (Barrère *et al.,* 2011).

The Barents Sea consists of numerous platform areas, basement highs, graben features and large sag-basins. The major structural elements are shown in Figure 2. Structurally, the Barents Sea shelf is characterized by ENE-WSW to NE-SW and NNE-SSW to NNW-SSE trends with local influence of WNW-ESE striking elements (Faleide *et al.*, 1984, Gabrielsen *et al.*, 1990, Gudlaugsson *et al.*, 1998).

According to Gabrielsen *et al.* (1990) and Smelror *et al.* (2009), the Barents Sea Shelf can be roughly divided into two main geological areas, which differ in their geological history. The eastern and northeastern parts are characterized by more stable platforms and less pronounced tectonic activity since the Late Carboniferous. In contrast, the western part is dominated by post-Caledonian rifting phases as well as later rifting episodes during the Cenozoic due to the opening of the North Atlantic (Gabrielsen *et al.,* 1990).

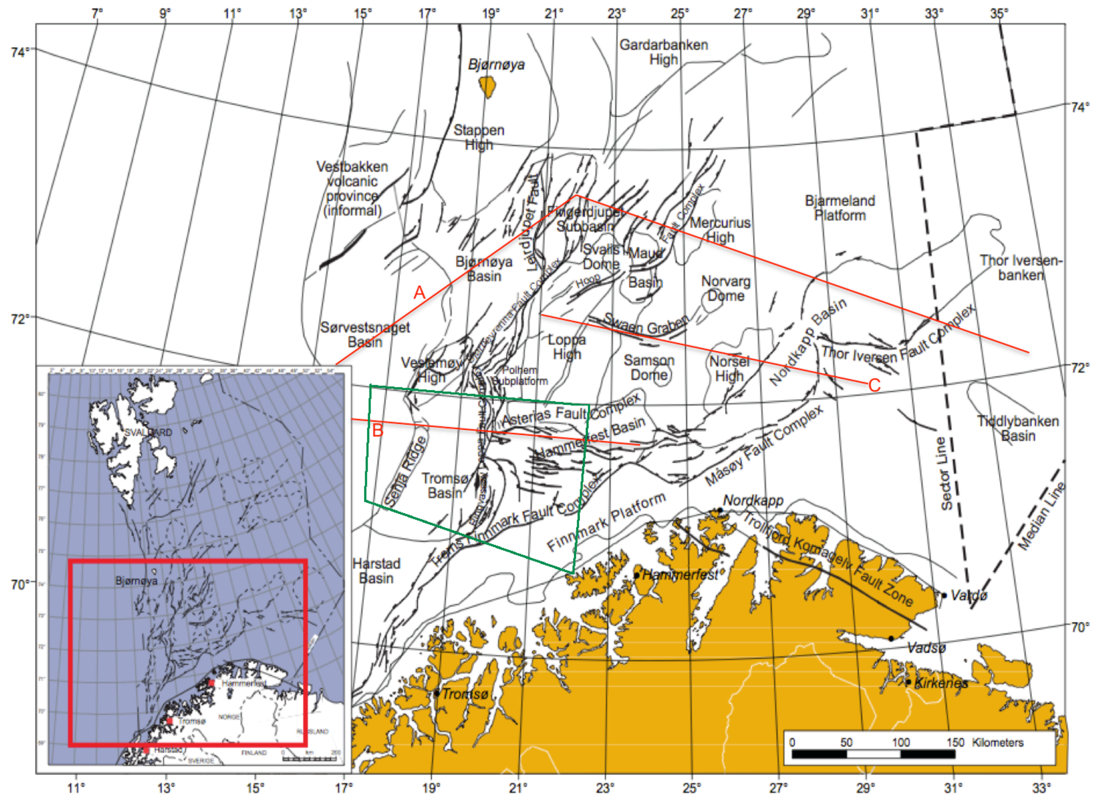

Figure 2. Map of the southern Norwegian Barents Sea showing main structural elements. Red lines display the location of regional profiles from Fig. 3. Green square shows location of study area (modified from Larssen *et al.*, 2005).

2.2 Western Barents Sea

The western Barents Sea Shelf consists of large thicknesses of Upper Paleozoic to Cenozoic rocks. Faleide *et al.* (1993) divided it further into three distinct regions: (1) The Svalbard Platform, which acted as a stable platform since late Paleozoic times and is covered by a relatively flat-lying succession of Upper Paleozoic and Mesozoic, mainly Triassic, sediments; (2) a basin province between the Svalbard Platform and the Norwegian coast. This region is characterized by a number of sub basins and highs with an increasingly accentuated structural relief westwards. The basin infill changes from Jurassic-Cretaceous sedimentary rocks to Paleocene-Eocene age sedimentary rocks towards the west; and (3) the western continental margin, which consists of three main segments (a) a southern sheared margin along the Senja-Fracture Zone; (b) a central rifted complex southwest of Bjørnøya associated with volcanism, and (c) a northern, initially sheared and later rifted margin and the Hornsund Fault Zone (Fig. 2). The continent-ocean transition occurs over a narrow zone along the line of Early Tertiary breakup and a thick Upper Cenozoic sedimentary wedge covers the margin.

2.2.1 Main structural elements in the southwestern Barents Sea

During the extensional history of the southwestern Barents Sea, several basins and intrabasinal highs have been developed. The structures are younger in the west and getting older towards the east. Figure 3 shows three profiles of the western Barents Sea, with the age of the sediment infill displayed by color. The location of the profiles is shown in Figure 2.

Two main provinces can be defined: (1) deep Cretaceous and Early Tertiary basins (Harstad -, Tromsø-, Bjørnøya – and Sørvestsnaget basins) separated by intrabasinal highs (Senja Ridge, Veslemøy High and Stappen High); and (2) Mesozoic basins (Hammerfest Basin) and highs (Finnmark Platform, Loppa High) which have not experienced the pronounced Cretaceous-Tertiary subsidence.

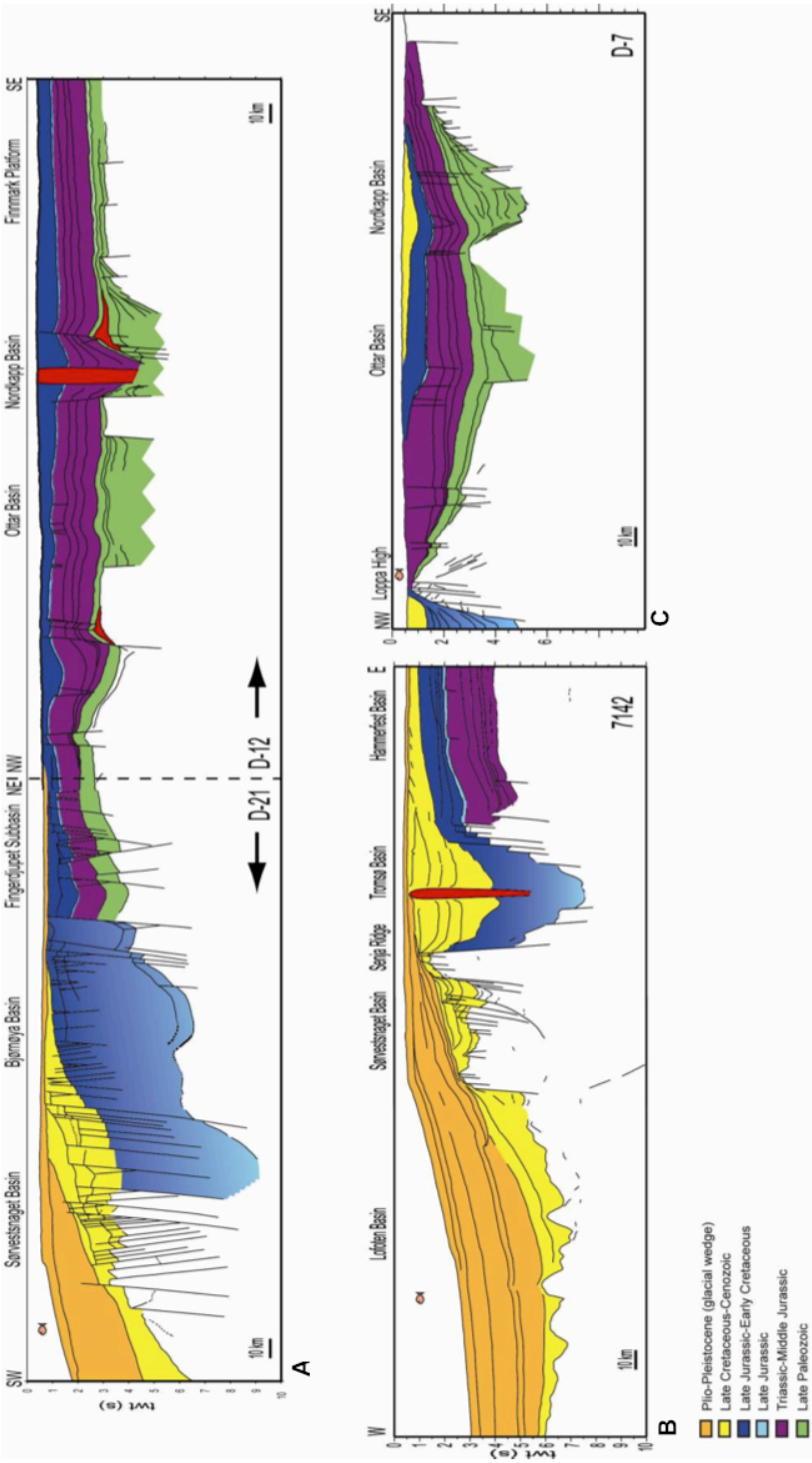

Figure 3. Regional profiles across the SW Barents Sea. Location of the profiles is shown in Fig. 2 (Faleide *et al*., 2009).

Continental boundary faults along the Senja Fracture Zone and east of the Vestbakken Volcanic Province form the western border of the continental shelf and the transition to the oceanic crust. Further east, major Jurassic-Cretaceous fault zones border the deep Cretaceous sedimentary basins; the Troms-Finnmark Fault Complex south of 71°N, the Ringvassøy-Loppa Fault Complex, the Bjørnøyrenna Fault Complex and the Leirdjupet Fault Complex (Faleide *et al*., 1993).

The Nordkapp Basin, on the eastern side of the western Barents Sea is a deep NE-SW striking basin of pre-Permian origin (Gabrielsen *et al.,* 1990). Northwest of it, lies the Ottar Basin, which is a deep NE-trending fault–bounded basin from the Late Paleozoic (Fig. 3c). Two large salt domes are present within the basin, the Norvarg Dome and the Samson Dome (Breivik *et al.,* 1995). The third main basin of Late Paleozoic age in this area is the Maud Basin, located between the Mercurius High in the northeast and the Loppa High in the southwest. The Maud Basin shows a NE, NNE trend and its evolution is probably related to the development of the pre-Permian Svalis Dome (Gabrielsen *et al.,* 1990).

The Hammerfest Basin is a relatively shallow basin, separated from the Finnmark Platform in the south by the Troms-Finnmark Fault Complex and from the Loppa High in the north by the Asterias Fault Complex (Gabrielsen *et al*., 1990, Larssen *et al.,* 2005). The Finnmark Platform south of the Hammerfest Basin forms a relatively stable segment and borders the Norwegian mainland in the south. It was characterized by rifting during the earliest post-Caledonian phases in the latest Devonian and Early Carboniferous (Samuelsberg *et al*., 2003). To the north of the Hammerfest Basin lies the Loppa High, a structural feature with a trapezoidal shape (Fig. 2; Gudlaugsson *et al.,* 1998). The Ringvassøy-Loppa and Bjørnøyrenna Fault Complexes bound the high in the west towards the Bjørnøya and Tromsø basins and in the east it grades gently towards the Bjarmeland Platform (Gabrielsen *et al*., 1990, Larssen *et al*., 2005).

A series of N-S to NE-SW trending fault complexes; e.g. the Ringvassøy-Loppa and the Bjørnøyrenna Fault Complexes, form the boundary between the older platform areas and highs in the east and the deeper, younger basins along the western margin of the Barents Sea (Larssen *et al*., 2005).

The Fingerdjupet Subbasin is the shallow, northeastern part of the Bjørnøya Basin, and separated from the Loppa High by the Bjørnøyrenna Fault Complex. Its formation took place during Early Cretaceous time, but the dominating fault trend was already generated during Late Jurassic time (Fig. 3a; Gabrielsen *et al*., 1997). The Leirdjupet Fault Complex towards the west of the Fingerdjupet Subbasin defines the margin to the NE-SW trending Bjørnøya Basin. Subsidence of this basin took place in the Early Cretaceous. Thus, most of the basin infill seems to be of Early Cretaceous age (Fig. 3a).
To the north, the Bjørnoya Basin is bounded by the Stappen High, which is a N-S elevated area, surrounding Bjørnøya as its highest point. It was a high during Late Paleozoic and Early Jurassic times, underwent subsidence during Mesozoic and became a positive element in the Tertiary again. (Faleide *et al*.,1993, Larssen *et al.,* 2005).

The Veslemøy High separates the Bjørnøya Basin in the north from the Tromsø Basin in the south. The NNE-SSW trending Tromsø Basin underwent large scale Cretaceous subsidence and sedimentation. Towards the west, the basin is constrained by the Senja Ridge, which was a positive structural element from Late Cretaceous to Late Pliocene and the formation has been related to strike-slip faulting along the Bjornøyrenna Fault Complex (Faleide *et al*., 1993). South of the Tromsø Basin lies the Harstad Basin, which was also characterized by significant subsidence during the Cretaceous (Gabrielsen *et al*., 1990).

The Sørvestsnaget Basin is situated on the western border of the Barents Sea. This basin represented a structural continuation of the Bjørnøya Basin during Cretaceous, but was later affected by major tectonics during the Tertiary breakup (Fig. 3a, b). Towards the north it is defined by the Vestbakken Volcanic Province (Faleide *et al*., 1993, Gabrielsen *et al.,* 1990).

2.3 Regional geology of area of investigation

2.3.1 Hammerfest Basin

The Hammerfest Basin is a fault-bounded, E-W extending relatively shallow feature. It was probably established in Late Carboniferous, although the main subsidence occurred in Jurassic to Early Cretaceous time. The basin is separated from the Finnmark Platform to the south by the Troms-Finnmark Fault Complex, and from the Loppa High to the north by the Asterias Fault Complex. The Ringvassøy-Loppa Fault Complex marks the boundary to the Tromsø Basin in the west. To the east, the relief of the basin gradually dies out as it gets narrower and shallower (Faleide *et al.,* 1984, Gabrielsen *et al*., 1990).

A gentle central dome, located along the basin axis and an internal fault system composed of E-W and WNW-ESE trending faults, reflecting predominantly the Late Jurassic tectonism and characterizing the internal structure of the basin. No evidence of extensive Late Paleozoic evaporite deposition or of diapirism is found in the basin, which is in contrast to the Tromsø Basin in the west. (Larssen *et al.,* 2005).

2.3.2 Tromsø Basin

The deep NNE-SSE trending Tromsø Basin is located west of the Hammerfest Basin and is separated by the Senja Ridge from the Sørvestsnaget Basin.

The Tromsø Basin is characterized by a thick sequence of Paleozoic salt and likely developed before the deposition of the evaporites. Main evolution of the basin took place during Late Jurassic-Early Cretaceous extension. Halokinesis played also an important role in the structuring of the Tromsø Basin. Several salt diapirs occur along the axis of the basins and the halokinesis has also been used to explain the extreme subsidence in Cretaceous times (Faleide, *et al*., 1993, Gabrielsen *et al.,* 1990). However, more recent studies show that salt movement occurred even in Paleogene (Ryseth *et al*., 2003).

3. Geological History

3.1 Paleozoic development

The Caledonides form the metamorphic basement of the western Barents Shelf. This orogeny developed during Late Silurian to Early Devonian due to a collision of the Laurentia and Baltica plates to form the Laurassian continent, following the closure of the Iapetus Ocean (Smelror *et al.,* 2009).

Old, inherited structures of the Caledonides show a NE trend in the southwestern Barents Sea and determine the pattern for younger extensional events (Dengo & Røssland, 1992, Faleide *et al*., 1984). Gabrielsen *et al.* (1990) stated that it is likely that older fracture systems are preserved in the basement underlying the sediments of the continental shelf, and that they have influenced the Late Paleozoic to Cenozoic structural development in the Barents Sea.

Following the Caledonian orogeny in Late Devonian times, the western Barents Sea was gradually eroded (Henriksen *et al.,* 2011). The erosion led to the deposition of thick continental clastic sediments, e.g. the Upper Devonian-Lower Carboniferous beds of the Billefjorden Group (Smelror *et al.,* 2009, Worsley, 2008).

In Late Devonian to Early Carboniferous, the tectonic regime changed to an extensional regime, possibly partly determined by a left-lateral shear regime with large-scale strike-slip movements (Faleide *et al*., 1984, Ziegler, 1978). The change of stress-regime is related to the initiation of the Atlantic rift system between Norway and Greenland. This rift-phase resulted in several interconnected rift basins filled with syn-rift deposits. The Tromsø, Bjørnøya, Nordkapp, Fingerdjupet, Maud and, possibly also, the Hammerfest Basin may have been formed during this time (Gudlaugsson *et al.*, 1998, Henriksen *et al*., 2011).

By the end of Carboniferous time, fault movements ceased in the eastern part and most of the Barents Sea had become a stable platform. Due to marine transgression in the Bashkirian, the rapidly subsiding basins became areas of deeper water deposition. The slowly subsiding highs were sites of shallow marine deposition from mid-Carboniferous until Late Permian. The regional sea level rise occurred in a time when the Earth's system was characterized by icehouse conditions and high frequency and amplitude fluctuations of sea level driven by glaciations in the southern hemisphere (Stemmerik & Worsley, 2005).

The northward drift of the shelf of around 2-3 mm/yr, from 20°N to 45°N paleolatitude during Carboniferous and Permian resulted in a climate shift from tropical humid to semi-arid and arid (Smelror *et al*., 2009, Stemmerik & Worsley, 2005). This, and the gradual drowning of the Barents Shelf, led to the development of a widespread carbonate platform in the Late Carboniferous-Early Permian, extending from the Sverdrup Basin to the Perchora Basin. Warm-water carbonates of various facies, evaporites and other clastics belonging to the Gipsdalen Group were deposited with a relatively even thickness, indicating a quiet tectonic period for that time in most of the area (Faleide *et al.,* 1984). Halite deposition took place in deeper basins during major sea level low-stands, when platforms were subaerially exposed and the basins were partly or totally separated from the open sea (Smelror *et al*., 2009).

In Mid-Late Permian times, dramatic changes in the depositional environment occurred on the Barents Shelf. The climate became cooler and changed from warm and arid to temperate. The seaway connection to the warm waters from the Tethys was closed. The deposition of carbonates ceased and was replaced by a siliciclastic regime. However, it was still a time of transgression and the Barents Sea was covered with an extensive marine shelf, dominated by a siliceous rich sponge fauna forming the deposits of the Tempelfjorden Group (Smelror *et al*., 2009). Structural highs acted as shallow marine highs and were also periodically exposed to the surface during sea level low stands in the Late Permian. In general, banks of bryozoans and brachiopods dominate the deposits (Henriksen *et al*., 2011, Johansen *et al*., 1994). In the western part, reactivation of mainly north-trending rift structures took place in Late Permian-Early Triassic (Gudlaugsson *et al.*,1998).

3.2 Mesozoic development

3.2.1 Triassic

In the southwestern Barents Sea the Triassic was generally a period of low tectonic activity, characterized by a passive regional subsidence. Minor movements occurred on the Finnmark and Bjarmeland Platforms, but more active fault movement was found along the western margin. Due to rifting west of the Loppa High, the high was uplifted and eroded in Early Triassic times (Smelror *et al.*, 2009). Further, the Triassic in this area is marked by the deposition of large clinoforms extending over the Hammerfest Basin and on to the Bjarmeland Platform, the oldest of which are of Induan age. These large-scale clinoforms probably represent sands, siltstones and shales sourced from the Fennoscandian hinterland and the Urals and deposited in delta-front to shoreface environments along the NE-SW trending paleocoastline. By this time, marine conditions existed in the western Barents Sea, where the deepest parts probably stretched through the Hammerfest Basin and across northern parts of the Finnmark Platform (Henriksen *et al.*, 2011, Smelror *et al.*, 2009).

During the progressive infill of the Barents Sea the depositional direction changed from eastward thickening in Early Triassic to north-northeastward thickening in Mid-Late Triassic. The depositional direction was affected by the paleotopography (Glørstad-Clark *et al.*, 2010). By the beginning of the Carnian, the setting in the Barents Sea changed from transgression to regression and the Barents Sea is characterized by an extensive westward progradation of near-shore and coastal depositional environments. It is suggested that a widespread coastal plain probably stretched from Novaya Zemlya into the Hammerfest Basin and Fingerdjupet Subbasin (Smelror *et al.*, 2009). At the same time, the southern part of the Loppa High started to develop into a basin where mainly deposition of clastic material occurred. The deposited shales, silt- and sandstones belong to the Storfjorden Subgroup of the Kapp Toscana Group. The inversion of the Paleozoic high to a basin indicates a significant change in stress regime and is considered to be caused by renewed extension in the North Atlantic rift system between Norway and Greenland (Glørstad-Clark *et al*., 2010). In the Norian a supra-regional relative sea level rise led to a change in depositional systems. The rate of subsidence and sedimentation decreased greatly in comparison to the earlier Triassic regimes. Basinal areas, like the Hammerfest Basin have been areas with more continuous sedimentation in comparison to structural highs and platforms. Shallow marine and coastal environments of the early Realgrunnen subgroup were established (Worsley, 2008).

3.2.2 Jurassic

As stated by Smelror *et al.* (2009), large areas of the Barents Sea were uplifted and eroded during the Late Triassic-Early Jurassic. In the Hettangian-Simurian times a regional regressive maximum occurred and the western and central parts of the Barents Sea, including the Loppa High and Svalbard, consisted of wide continental lowlands. Sandy sequences assigned to the Tubåen Formation were deposited in the Tromsø, Hammerfest and Nordkapp basins. The formation represents mostly tidal inlets, estuaries and lagoons.

In general the southern Hammerfest Basin was a major depocenter during that time, and the main provenance area was probably located on the Fennoscandian mainland.

After the domination of the low-lying floodplain environment in latest Early Jurassic in the southwestern Barents Sea, a global sea level rise during Toarcian led to a change to more prograding coastal settings and sandstones, siltstones and shales of the Stø Formation were deposited in the Hammerfest, Nordkapp and Bjørnøya Basins. Towards the Late Toarcian, shallow-marine environments occurred in this region.

In the beginning of Middle Jurassic another sea level fall occurred with its maximum regression in the Bajocian. According to Smelror *et al.* (2009), large parts of the shelf were exposed to erosion and a depositional gap is observed over most of the western Barents Sea. A major transgression at the Top of Oxfordian led to the depositon of fine-grained sediments over the most of the southwestern Barents Sea. The clays have been deposited in a deep marine environment with anoxic bottom conditions due to restricted circulation from the formation of local barriers (Worsley *et al*., 1988). The dark and organic rich shales form the source rock of the Hekkingen Formation.

Late Jurassic to Early Cretaceous times were a period with renewed crustal extension and minor strike-slip activity along old lineaments. The extension was caused by the Arctic-North Atlantic rift system that gradually opened during the Mesozoic leading to crustal separation between Greenland and Norway. (Faleide *et al*., 1984) The Middle-Late Jurassic rift propagated through the Hammerfest and Bjørnøya basins along the pre-existing tectonic structures. This led to a wide rift basin, regional block-faulting and differential subsidence in the Hammerfest, Tromsø and Bjørnøya basins (Faleide *et al*., 1993, Gabrielsen *et al*., 1990, Smelror *et al.,* 2009). The inherent northeastern structural trend controlled the tectonic patterns in the western Barents Sea. Exceptions are found in the Hammerfest Basin, where east-west trending faults are superimposed on the older structural trends along the northwest boundary of the Hammerfest Basin with the Loppa High. Doming occurred in the Hammerfest Basin as a response to the movements on the basin´s boundary faults to the north and the south (Dengo & Røssland, 1992). The Stappen and Loppa Highs became positive structures at this time due to uplift, faulting and differential subsidence (Faleide *et al*., 1993).

The tectonic subsidence outpaces the deposition rate at the end of the Jurassic leading to a transgressional setting with its maximum in the Tithonian. Mostly shales and mudstones of the early Adventdalen Group were deposited, especially in the deep-water areas between the faulted blocks (Smelror *et al*., 2009).

3.2.3 Cretaceous

The transition from the Jurassic to the Cretaceous is dominated by a major rifting episode combined with a low-stand of sea level (Faleide *et al.,* 1993). The areas of marine sedimentation in the Barents Sea had been reduced, but an open connection to the Tethys in the southeast still existed (Smelror *et al.,* 2009).

In Early Cretaceous times, the rifting of the North Atlantic rift system extended into the southwestern Barents Sea. At least three tectonic phases affected the area during Early Cretaceous times. The first two phases occurred between Berriasian – Valanginian and between Hauterivian – Barremian and affected the Hammerfest Basin and also the basins further west. In early Barremian the doming in the Hammerfest Basin terminated which presents the end of the active rifting in this basin. During Aptian – Albian, tectonic activitiy is recognized again by uplift of the north-northeastern Barents Sea, which resulted in the erosion of large amounts of sediment. The Loppa High was uplifted relative to the subsidence of the Hammerfest Basin (Henriksen *et al.*, 2011), leading to erosion of the Jurassic and Triassic sediments when the high was emergent (Wood *et al*., 1989).

Additionally, subsidence increased in comparison to the Late Jurassic in the southwestern basins and reached its maximum during this period (Faleide *et al*., 1984). Due to the subsidence, which was particularly rapid along the Bjørnøya and Ringvassøy-Loppa Fault Complexes, the Bjørnøya, Harstad and Tromsø Basins became deep basins and main depocenters in the Barents Sea. The basins were filled by a 5-6 km thick sequence of the Kolmule Formation, which covered most of the structural relief by Cenomanian time (Faleide *et al*., 1993, Gabrielsen *et al*., 1997).

Worsley (2008) noted that a regional sea level rise in the Aptian cut off the coarse-clastic supply and led to the deposition of a shale-dominated wedge, thickening from Svalbard to the southwestern Barents Sea. In Late Cretaceous the general extensional setting may have prevailed regionally in the Barents Sea. The Tromsø Basin continued to subside, whereas the areas to the east are characterized by condensed sequences. Part of the differential subsidence may relate to salt movements causing the salt diapirs in the Tromsø Basin (Faleide *et al*., 1993). However, locally compressional deformation took place as well, leading to a second stage of inversion of depocenters in Late Cretaceous – Early Tertiary (Gabrielsen *et al*., 1997).

3.3 Cenozoic development

The evolution in the Cenozoic is closely related to the opening of the Norwegian - Greenland Sea beginning in the Late Paleocene (Henriksen *et al*., 2011). The continental break up of the Norwegian - Greenland Sea at the Paleocene-Eocene transition initiated the formation of the mainly sheared western Barents Sea-Svalbard continental margin which experienced both transtensional and transpressional deformation during Eocene times. The Senja Fracture Zone may have formed as a result of the transtension and at the same time, the transpressional regime caused a foreland fold- and thrust-belt on Svalbard (Faleide *et al*., 1993, Smelror *et al*., 2009). In Paleocene-Eocene times marine conditions prevailed in the Tromsø Basin, while at the same time sediments were shed into the basin from emergent highs in the east.

In mid-Oligocene a shift of tectonics took place and uplift and erosion of the margin and shelf areas occurred and the sedimentary wedges were prograding further towards the west (Faleide *et al*., 1993, Ryseth *et al*., 2003). A Pliocene unconformity occurs between the Mesozoic-Tertiary strata and the overlying glacial deposits in the Barents Sea. This marks the beginning of the Northern Hemisphere glaciations in the Late Pliocene.

The Barents Shelf was covered by ice during three major phases. The repeated glaciations caused isostatic uplift after deglaciation and erosion. Around Svalbard and the northern platform areas the uplift and erosion was at a maximum of 2-3 km. Further south in the Hammerfest and Nordkapp basins and on the Loppa High, the amount of uplift and erosion was in general less than 2 km (Smelror *et al*., 2009). The eroded sediments were transported to the shelf-margin and up to 5 km of fine-grained deposits of the Nordland Group have been deposited along the western margin, e.g. in the Sørvestsnaget and Lofoten Basin or spilt over onto the newly formed oceanic crust (Fig. 3; Faleide *et al.,* 1996, Worsley, 2008).

4. Work Area and Database

4.1 Seismic database

The seismic database for this study consists of 13 2D seismic lines covering the area of investigation in the Hammerfest and Tromsø basins (Fig. 4). The selected seismic lines belong to the published seismic database hosted by the Norwegian Petroleum Directorate (NPD) and are listed in Table 1. Thanks to AGR Oslo for processing and providing the herein used data.

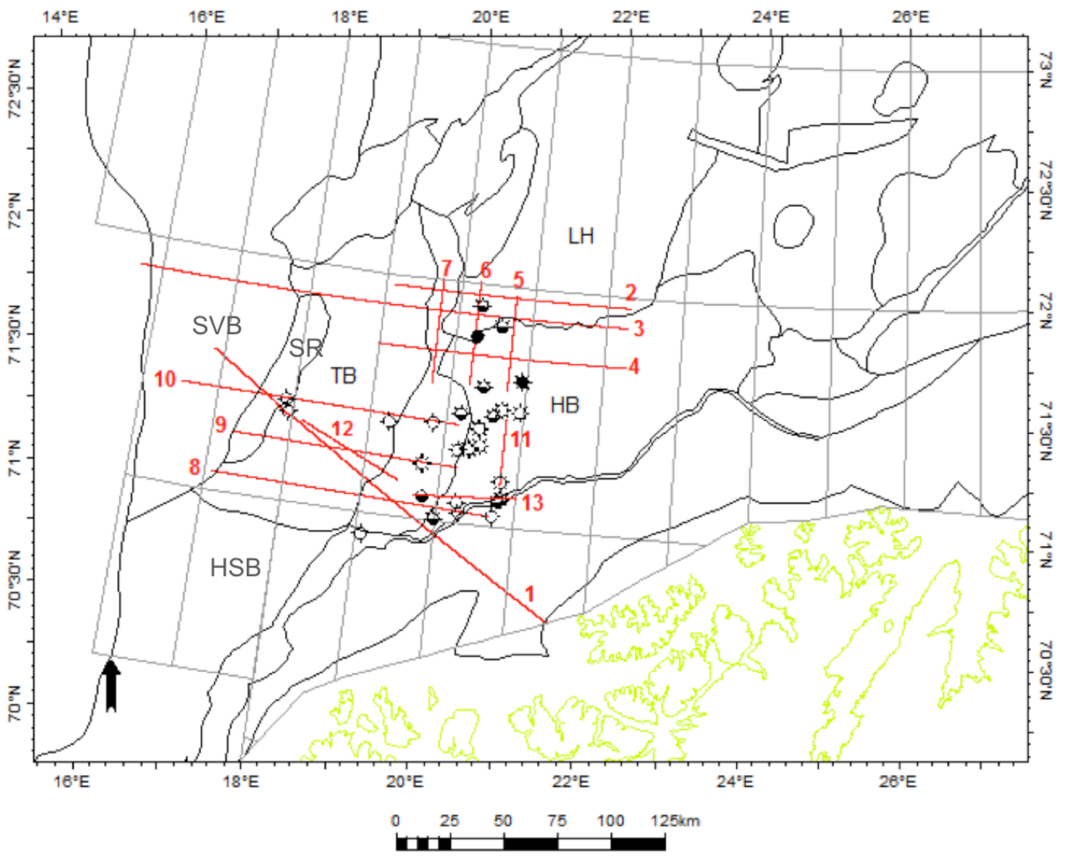

Figure 4. Overview of the study area with structural elements (black lines), seismic lines (red lines) and wells (black symbols). Numbers 1-13 refer to the seismic lines listed in Table 1 (LH = Loppa High, HB = Hammerfest Basin, HSB = Harstad Basin, SR = Senja Ridge, SVB = Sørvestsnaget Basin, TB = Tromsø Basin).

4.2 Well data

Well data of 28 wells located in the area of investigation were provided by AGR. The well top picks of the wells were used for the seismic interpretation in this study to link the seismic interpretation with the wells. In areas, which were devoid of seismic data, though with wells present, the well tops were used to infill the seismic interpretation. Check shot velocities from well data have been used to calibrate the velocity model for the depth conversion. The selected wells are listed in Table 2.

4.3 Stratigraphy

All stratigraphic terms used in this report follow the official definition given by Mørk *et al.* (1999), Worsley *et al.* (1988) for the Mesozoic and Cenozoic successions. For the Paleozoic time sequence the nomenclature follows Larssen *et al.* (2005). Figure 5 shows the generalized stratigraphy for the western Barents Sea as well as an overview about the interpreted and constructed horizons utilized in this study.

Table 1.

Selected seismic lines from NPD database.

(1) NPD-TR-82_MIG_RAW D-2-82	(8) NH9703_DO22_MIG_FIN
(2) NPD-TR-82_MIG_RAW 7157-82	(9) NH9703_DO20M_MIG_FIN
(3) NPD-TR-82_MIG_RAW 7152-82	(10) NH9703_DO19M_MIG_FIN
(4) NPD-TR-82_MIG_RAW 7142-82	(11) NH8250_FINMIG_3041
(5) NPD-TR-82_MIG_RAW 2045-82	(12) NH8103_RawStk_824
(6) NPD-TR-82_MIG_RAW 2015-82	(13) T-89_MIF_FIN-203
(7) NPD-TR-82_MIG_RAW 1945-82	

Note. Numbers 1-13 indicate the location of the seismic lines in Figure 4.

Table 2.

Selected wells in the study area.

Block 7019	Block 7117	Block 7119	Block 7120	
7019/1-1	7117/9-1 7117/9-2	7119/7-1 7119/9-1 7119/12-1 7119/12-2 7119/12-3	7120/1-1, R&R2 7120/1-2 7120/2-2 7120/5-1 7120/6-1 7120/7-1 7120/7-3 7120/8-1 7120/8-2	7120/8-3 7120/9-1 7120/9-2 7120/10-1 7120/10-2 7120/12-1 7120/12-2 7120/12-3 7120/12-4

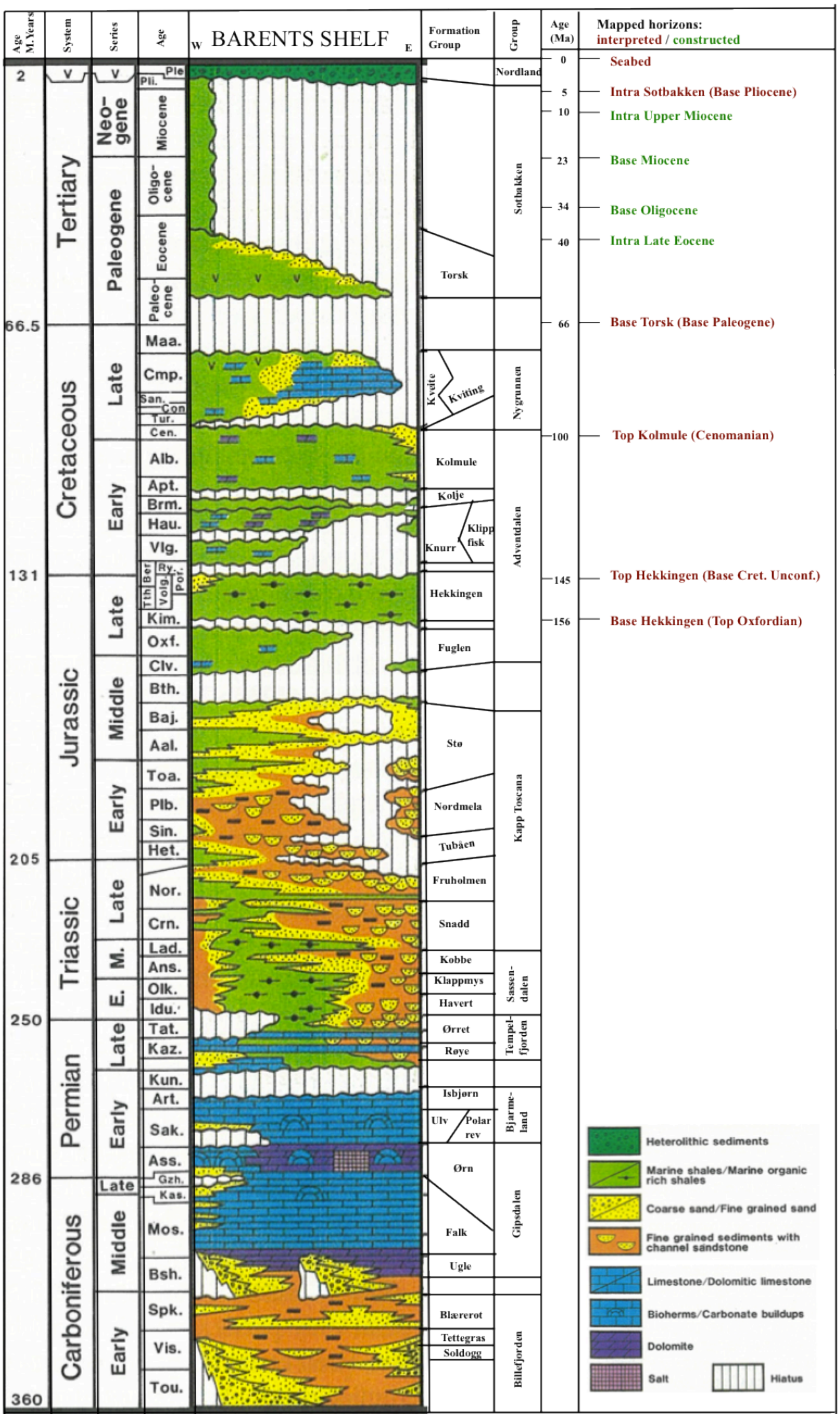

Figure 5. Generalised litho- and chronostratigraphy for the western Barents Sea and mapped horizons (modified after Nøttvedt *et al.*, 1992).

5. Seismic Interpretation – Time Maps

Prior to the reconstruction of the paleobathymetry, the objective of this part of the project was to produce time maps by interpreting the seismic data. In total, six horizons were interpreted in the work area, based on the seismic database and the well top picks. As an approach for this interpretation, seismic stratigraphy was used. Additionally, time maps from the earlier accomplished IBS - BMU 2008 (Inthorn *et al.,* 2008) were utilized as support for the interpretation that was carried out with the software PETREL.

5.1 Seismic stratigraphy

Seismic stratigraphy is an approach to interpret reflection seismic within the geological framework and was first introduced by Vail *et al.* (1977). This method is based on the property that primary reflections are generated by velocity and density contrasts at physical surfaces in the rocks, consisting mainly of stratal surfaces and unconformities. The resulting interpreted seismic section is then the record of the chronostratigraphic depositional and structural patterns.

The main idea of seismic stratigraphy is the identification of stratigraphic units composed of relatively conformable successions of genetically related strata, termed depositional sequences (Fig. 6). These are bounded at the top and base by an unconformity or its correlative conformity.

An unconformity is a surface separating older from younger strata representing an episode of erosion or non-deposition. The missing interval is called a hiatus. There are three kinds of unconformities: disconformity, nonconformity and angular unconformity. A conformity separates older from younger strata without any evidence of erosion or non-deposition.

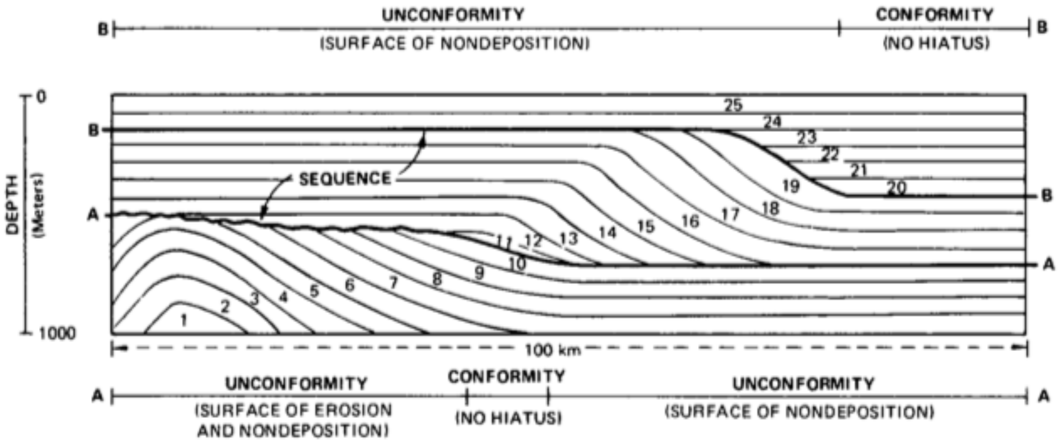

Figure 6. Schematic illustration of a depositional sequence (Vail *et al*., 1977).

Depositional sequence boundaries can be recognized by the termination of reflections caused by lateral terminations of strata, called discordant surfaces. Three main types of discordance at upper and lower boundaries can be identified and are described below. Concordance can be understood as a reference of continuous sedimentation. The sediments lying on top of each other have the same strike and dip (Fig. 7).

Lower boundary:

Onlap: is a base-discordant relation in which initially horizontal strata terminated against an initial inclined surface or in which an initially inclined strata terminates against a surface of greater inclination.

Downlap: is a base-discordant relation in which initially inclined strata terminates down-dip against an initially horizontal or inclined surface.

Upper boundary:

Toplap: is the termination of strata against an overlying surface mainly as a result of non-deposition or sediment bypassing with perhaps minor erosion.

Erosional truncation: is the lateral termination of a stratum against the upper boundary of a sequence caused by erosion. This type is common where strata are tilted by structural movements.

Structural truncation: is the lateral termination of a stratum by structural disruption, produced by faulting, gravity sliding, salt flowage or igneous intrusion.

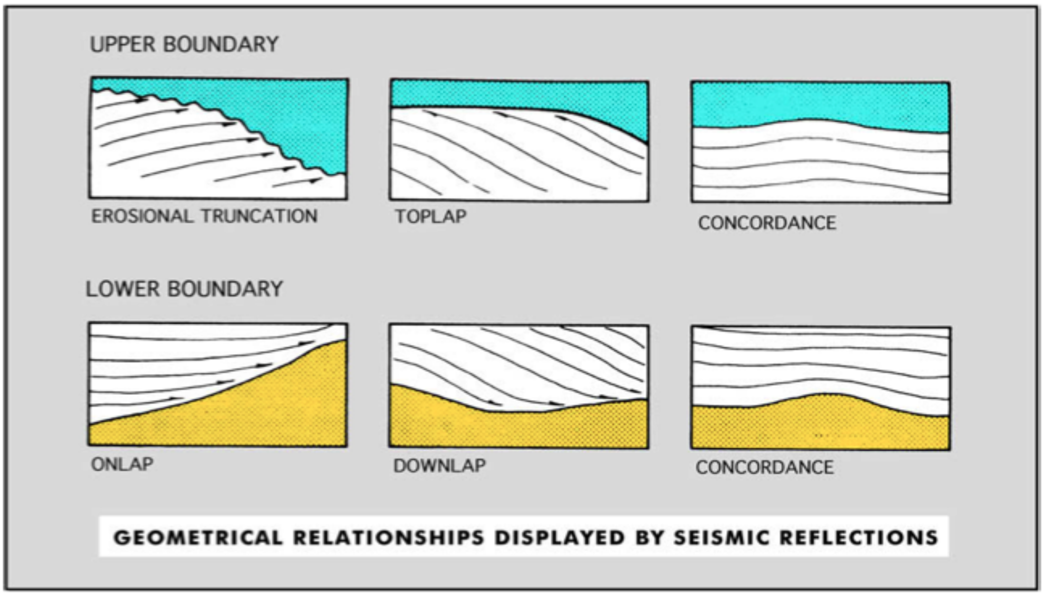

Figure 7. Various types of unconformable relationships displayed by the reflection geometries on seismic sections (Veeken, 2007).

5.2 Interpreted horizons - time maps

Based on the seismic database six horizons have been interpreted in the area of investigation. To find the relation between the seismic reflections and the stratigraphy well top information has been used. Additionally, interpretation of major faults has been carried out to represent the main structures in the area. The six interpreted horizons are described below and the interpretation on seismic line T-89_MIF_FIN-203 is shown as an example in Figure 8.

Seabed: was interpreted on the seismic on a strong negative reflector over the whole area.

Intra Sotbakken/Base Pliocene: was picked on the seismic as a distinct unconformity displaying the Base Pliocene. The Sotbakken Group consists of many local subsequences, which made it difficult to identify the Top Sotbakken, so an Intra Sotbakken horizon was interpreted.

Base Torsk/Base Paleogene: was identified in the Hammerfest Basin as a mainly strong reflector representing the top of the Late Cretaceous Nygrunnen Group. In the north the horizon is terminated towards the Loppa High Fault

Complex. In the western part of the mapped area, structural complexity and low data coverage made it difficult to follow the horizon.

Top Kolmule: represents the boundary between the Adventdalen and Nygrunnen Group. The reflector was recognizable in the Hammerfest Basin and the correlation with well tops supported the interpretation.
In areas where only a few or no wells have been available, it was difficult to track the horizon.

Top Hekkingen/BCU: marks the Base Cretaceous Unconformity representing the top of the organic rich Hekkingen shale. On some seismic lines it could be picked as a strong reflector and was also utilized for fault interpretation. In the northwest it terminates against the Loppa High. No strong reflector could be tracked in the deeper areas west of the Ringvassøy-Loppa Fault Complex due to reduced quality of the seismic and lack of well data.

Base Hekkingen: represents the boundary of the organic rich Hekkingen shale to the underlying mudstones from the Fuglen Formation. In the western parts of the mapped area it was not possible to pick a specific seismic event due to low data coverage and reduced quality of the seismic.

The final interpretations of the horizons have been used to generate the initial time maps with the Make Surface panel in PETREL. These surfaces will be used later as an input in the Geomodel.

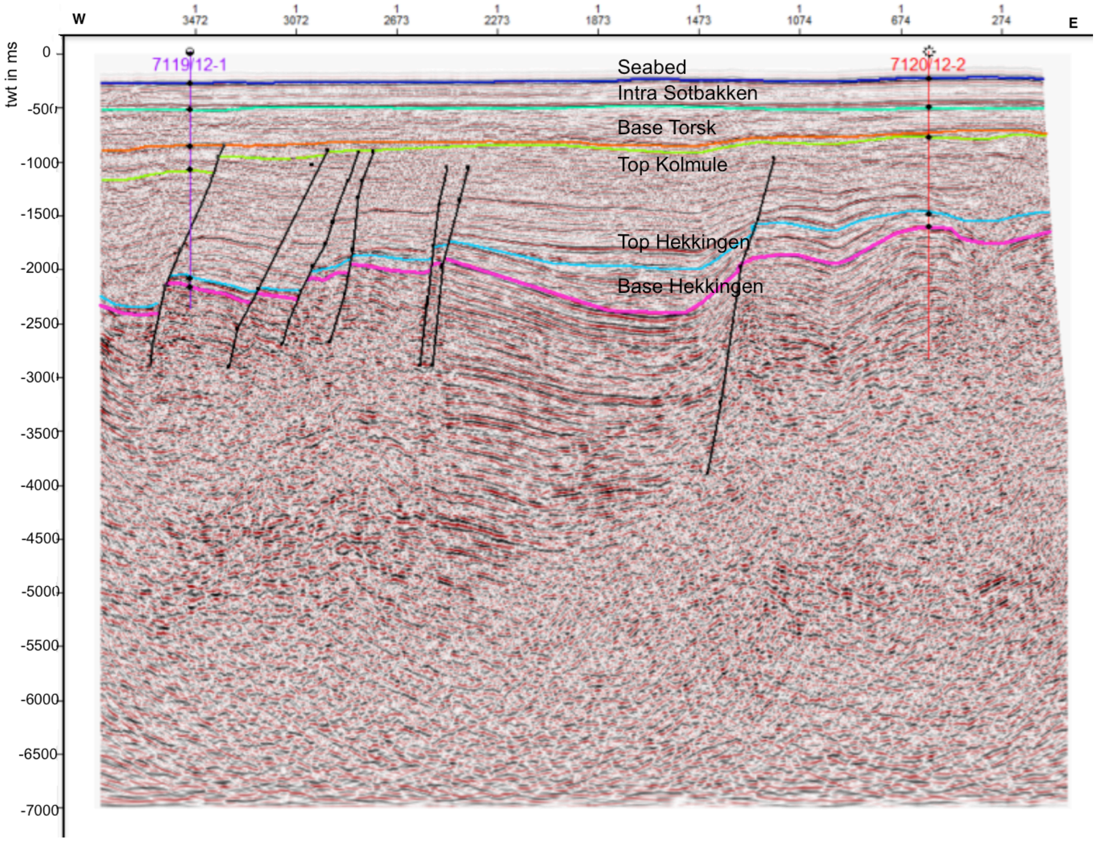

Figure 8. Interpretation of line T-89_MIF_FIN-203.

6. Geomodel

6.1 Geomodel building

The next part of this study was to build a Geomodel, a 3D grid representing the horizons and faults. The purpose of this was to get surface maps of the 6 horizons, which include the structural settings of the area. Therefore the following 3 steps have been carried out in PETREL:

Fault modeling

In the fault modeling process, the previous interpreted faults were digitized by generating "key pillars". These key pillars define the shape of the faults that should be modeled in the 3D grid (Fig. 9). In addition to the interpreted faults, two circular faults have been modeled around the salt diapirs in the Tromsø Basin, in order to represent them in the 3D grid. The final fault model was extended to and/or cut by the bottom and top horizon, which were in this case Base Hekkingen and Intra Sotbakken.

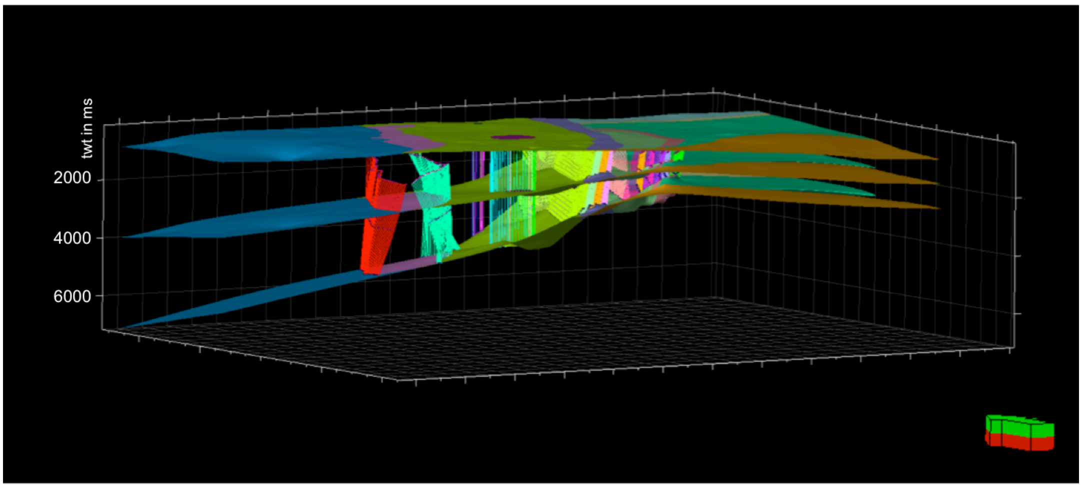

Figure 9. 3D grid over the study area including the modeled faults, displayed with key pillars (x:y:z=1:1:10).

Pillar Gridding

The next step was the Pillar Gridding process, which defines the "skeleton framework" for the 3D grid. The interpreted faults have been assigned to x and y directions according to their location in the grid. This was done to guide the gridding process and to orient the cells of the grid parallel to the faults.

Additionally, x and y trends have been defined in the grid to support the reconstruction of the structural patterns. The main faults and trends delimiting the tectonic units were defined as segment boundaries. The result was a 3D grid, representing the main segments in the studied area (Fig. 10).

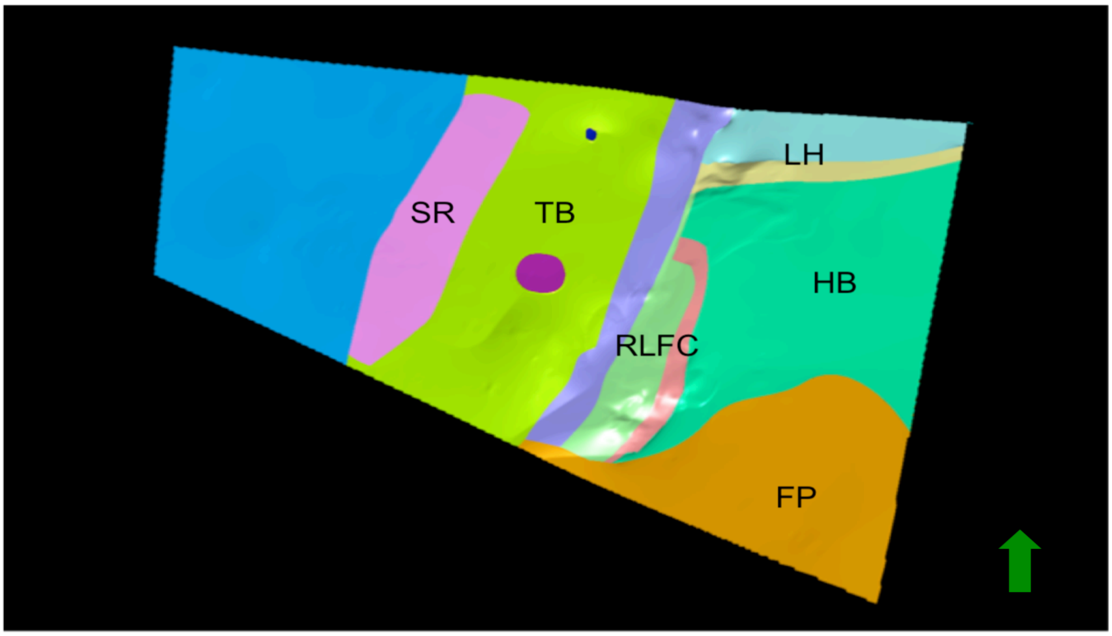

Figure 10. View from above on the 3D grid, representing the main segments of the studied area after the Pillar Gridding process (FP = Finnmark Platform, HB = Hammerfest Basin, LH = Loppa High, RLFC = Ringvassøy-Loppa Fault Complex, TB = Tromsø Basin, SR = Senja Ridge)

Make Horizons

In the following Make Horizon process, horizons have been generated to fill in the 3D grid. The previously created time surfaces served hereby as an input. The horizon types were set to conformable and minimum curvature interpolation method was used. Settings were taken over from Inthorn *et al.* (2008). The final horizons were converted to surfaces, which now represent time maps of each interpreted horizon including the structural setting from the fault model.

The low 3D data coverage in the area of investigation led to the generation of peaks and holes in some of the maps during the Make Horizon and gridding process. These errors have been edited manually by removing the peaks and smoothing the map with the Edit surface/polygon panel in PETREL.

6.2 Uncertainty

The accuracy of the time maps is depending on several factors such as the quality and quantity of the input data, the interpretation and gridding process.

Sparse data distribution of seismic lines has an influence on the accuracy of the map generation. Especially in areas with changing topography and structural complexity, one can miss important topography details due to the low 3D data coverage. The accuracy of the interpretation on the seismic line itself depends on the seismic data quality and investigation depth. The uncertainty of the interpretation increases in areas with a lot of noise or poor seismic responses due to increasing depth.
In areas with less or no well coverage it is difficult to select and follow the right seismic event during the interpretation process, especially when new sub-sequences appear in that area.

How well the gridding process recreates the input data and thereby the topography is dependent on the gridding techniques (e.g. grid size, interpolation method) and the complexity of the topography. Due to prior experiences a grid size of 250 x 250 was selected for the maps in this study. A higher grid resolution led to artifacts and too long calculation times. The grid cell dimension should be selected on the spatial distribution of the input data. Minimum curvature was used as an interpolation method giving smooth surfaces and attempting to honor the input data.

7. Depth Conversion – Depth Maps

Depth conversion is the process of transforming the seismic data from time domain into depth domain through a velocity model. The principle of depth conversion is based on the basic velocity – travel time relation valid for zero-offset, shown in the following equation, d (m) is the depth, v (m/s) is the velocity and twt (s) is the two-way-travel time (1) (Sheriff & Geldart, 1995):

$$d = \frac{v \cdot twt}{2} \qquad (1).$$

In this work, the depth conversion of the generated time maps from the 3D grid was accomplished in PETREL after generating a velocity model.

7.1 Depth conversion

Building the velocity model during this study was an iterative process, where several changes of the input data have been applied to minimize the uncertainties of the depth conversion. In general, the results of the depth conversion in areas with low data coverage and major changes in geology will give a higher degree of uncertainty. Additionally, it is assumed that the uncertainty will increase with depth.

At first a simple block model was built based on the depth maps taken from Inthorn *et al.* (2008) and the simple velocity relation of equation (2). V_0 (m/s) is the surface or reference velocity and v_{int} (m/s) the interval velocity.

$$v = v_0 + v_{int}. \qquad (2).$$

Interval velocities for the horizons have been calculated using two-way-travel time and depths from the well top data. The low data coverage, particularly in the western part of the area and the lack of wells penetrating all interpreted formations, resulted in a velocity model with large discrepancies between the time and depth converted seismic. For the deeper horizons, e.g. Top Hekkingen, mis-ties up to 1000 m have been found.

In the next step, several velocity models were built based on the instantaneous velocity function, where v_t (m/s) describes the increase in velocity with time, t (s) (3).

$$v_t = v_0 + k \cdot t \qquad (3).$$

V_0 (m/s), the surface or reference velocity and k (s^{-1}), the acceleration term, give a description of how the instantaneous velocity changes with time (Smallwood, 2002). In the first models v_0 and k were set constant and well tops were used for the correction of the model.

The correction with well tops resulted in higher errors, so it was not applied any further. Instead of the constant values for v_0 and k, the values were taken from check-shot data. This led to an improvement of the velocity model and reduced the mis-ties between the well tops and the seismic lines in time and depth domain. Before using the well velocity data, the two-way-travel time was plotted as a function of interval velocity (Fig. 11). The plot should show a trend of increasing interval velocity with increasing two-way-travel time. Distinct outliers were removed.

The final velocity model utilizes the time maps generated after the Geomodel process as a base, and follows the velocity equation (3) with values for v_0 and k taken from the check-shot data. The agreement between the well tops and the seismic in time and in depth domain has been checked and the mean deviation for each horizon after depth conversion is shown in Table 3. The mean deviation is increasing with depth as it was assumed beforehand. However, the values are acceptable for each horizon, showing that the depth conversion gives a satisfactory output and that the generated depth maps can be used further in this study.

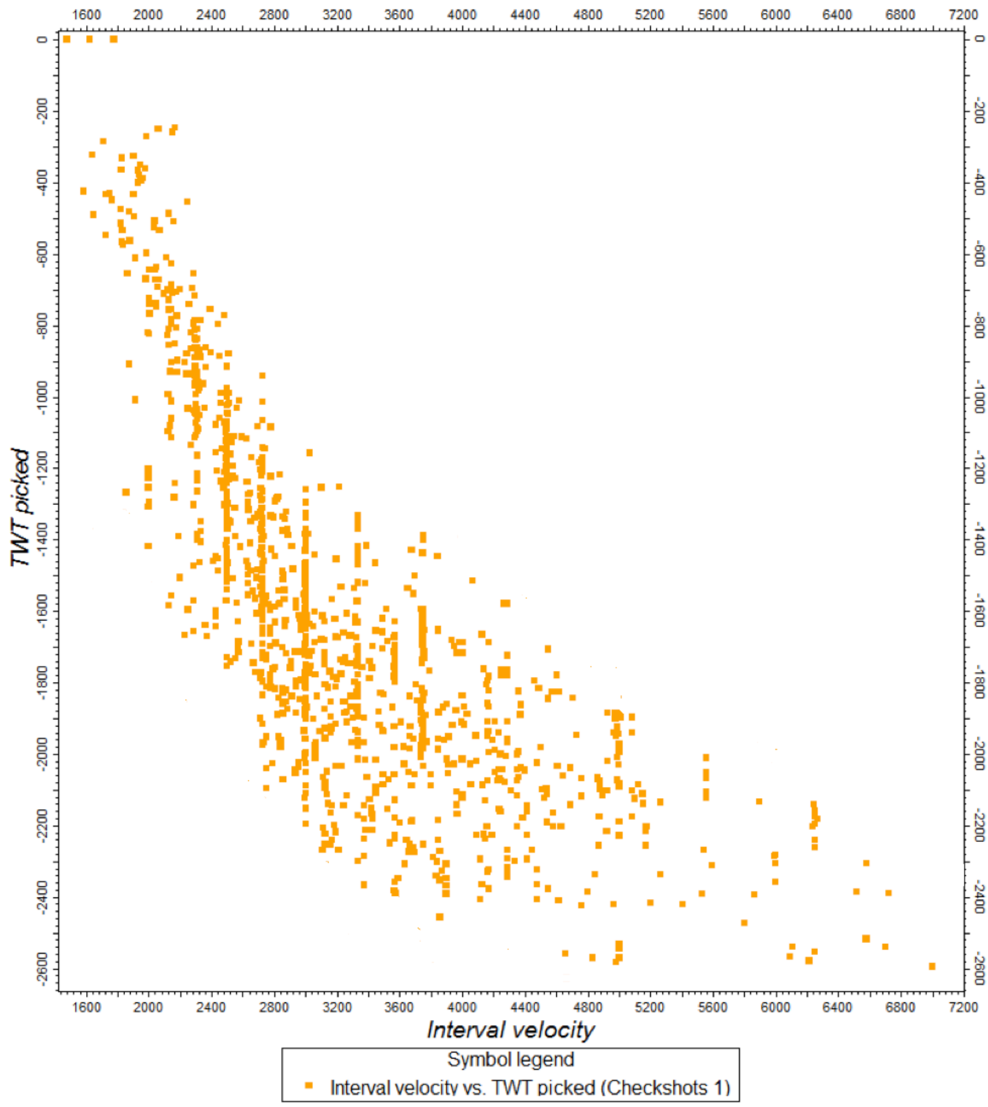

Figure 11. Plot of interval velocity (m/s) vs. two-way-travel time (ms).

Table 3.

Mean deviation of depth converted seismic data to the well tops.

Horizon	Number of well tops (n)	Mean deviation (m)
Seabed	6	5
Intra Sotbakken	6	14
Base Torsk	6	20
Top Kolmule	6	25
Top Hekkingen	6	40
Base Hekkingen	5	53

Note. N, number of well tops is the number of well tops used for the calculation of mean deviation because they intersect with a seismic line.

7.2 Depth maps

The generated depth maps have been compared to the initial time maps to check for discrepancies. Discrepancies can occurred due to lack of wells or check-shot data in some areas. This can cause errors in the velocity model due to insufficient input data.

A discrepancy was found on the Base Hekkingen map in the southwestern area on the Finnmark Platform. This area was lowered around 400 - 700 m and the distinct boarder to the Hammerfest Basin was not visible anymore in the depth map. The error might be due to the fact that the well database did not include any wells in this area, which could be used for the depth conversion.

To reduce the error, several dummy wells have been created on the Finnmark Platform along the border to the Hammerfest Basin. Well data were taken from a nearby well, located further west on the Finnmark Platform. The new wells have been included in the velocity model, but the renewed depth conversion did not show much improvement. This might be because the check-shot data could not be integrated into the dummy wells.

Another possibility was to elevate the area manually. Therefore the well top data from a nearby well on the Finnmark Platform and the Base Hekkingen depth map from Inthorn *et al.* (2008) have been used as reference points.

A further problem was that the detailed structural features of the Senja Ridge were not represented in the Base Torsk and Top Kolmule surfaces based on the sparse seismic data distribution. However, the N-S trend of this feature was observable. It is known that the Senja Ridge as a positive feature developed in the Paleogene (Ryseth *et al.,* 2003). Therefore the formation of the Senja Ridge influenced the older horizons as well and similar structures should be observable. In the initial maps of Base Torsk and Top Kolmule the Senja Ridge was only mapped in the southern part of the study area. Hence, it was elongated manually applying geological understanding and according to its trend towards the north in the Base Torsk and Top Kolmule surfaces.

The low quality of the seismic data in the deeper parts meant that the salt diapirs in the Tromsø Basin and the Senja Ridge were not represented by the interpretation of the Top and Base Hekkingen horizons and are consequently not present in the maps of Top and Base Hekkingen. For this reason a relative thickness factor was calculated between the overlying Base Torsk and the Top Hekkingen surfaces along a line in an area where the seismic interpretation still existed for both horizons. Then the Base Torsk surface was copied and multiplied with the relative factor. Subsequently, the area of interest around the structural features was cut by a polygon and merged with the Top Hekkingen depth map. The constructed surface represented the Senja Ridge and the salt diapir structures incorporated in the Top Hekkingen horizon (Fig. 12).

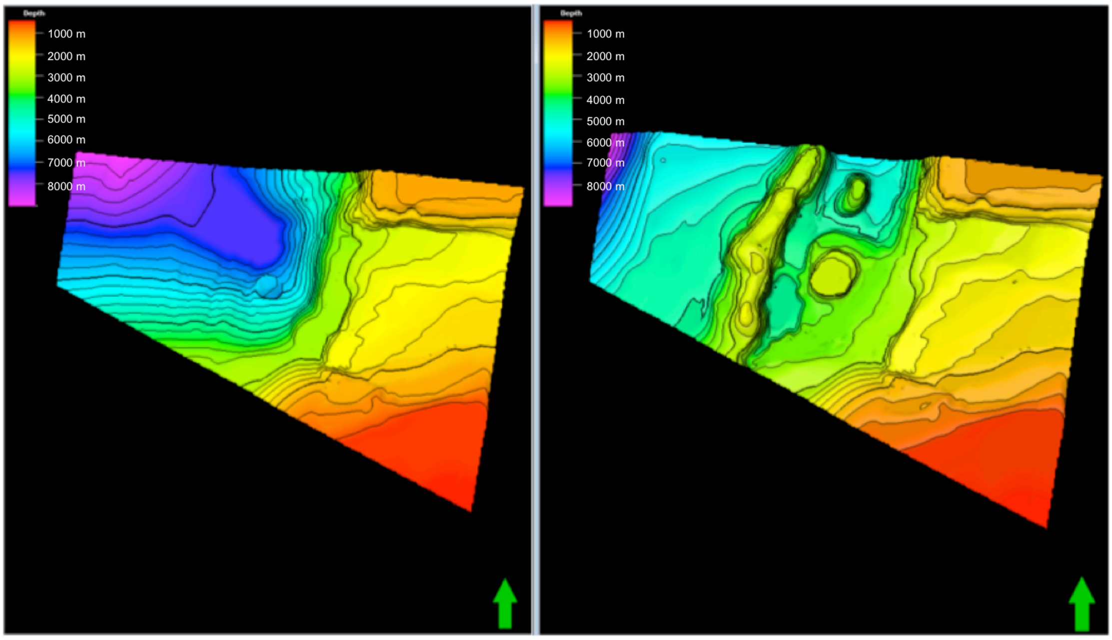

Figure 12. Left side: Top Hekkingen depth map without structural features of Senja Ridge and the salt diapirs in the Tromsø Basin. Right side: Structural features are integrated in Top Hekkingen depth map.

However, the area should be handled with care in further work, because it might not represent the actual geology and depth of the horizon.
The same procedure was applied to the Base Hekkingen surface.

In addition to the interpretation-based maps, four extra maps were constructed based on Ryseth *et al.* (2003) and conceptual thickness assumptions. The maps were constructed for Intra-Upper Miocene, Base Miocene, Base Oligocene and Intra Late Eocene. The thickness fraction of each of the surfaces was multiplied with the isopach map of Intra Sotbakken – Base Torsk and then added to the Intra Sotbakken surface or the respective overlying surface.

In order to accomplish the paleobathymetry reconstruction for the Base Hekkingen horizon, a dummy horizon was constructed by making a copy of Base Hekkingen and increasing the depth by 200 m. This horizon is called Top Fuglen Dummy and an age 158 Ma was assigned.

Figure 13 shows a 3D view of the Geomodel with the 10 final horizons. The depth maps were exported for further use in the paleo-water reconstruction as IRAP classic binary grids with a grid resolution of 250 x 250 m. The depth maps for each horizon can be found in the Appendix.

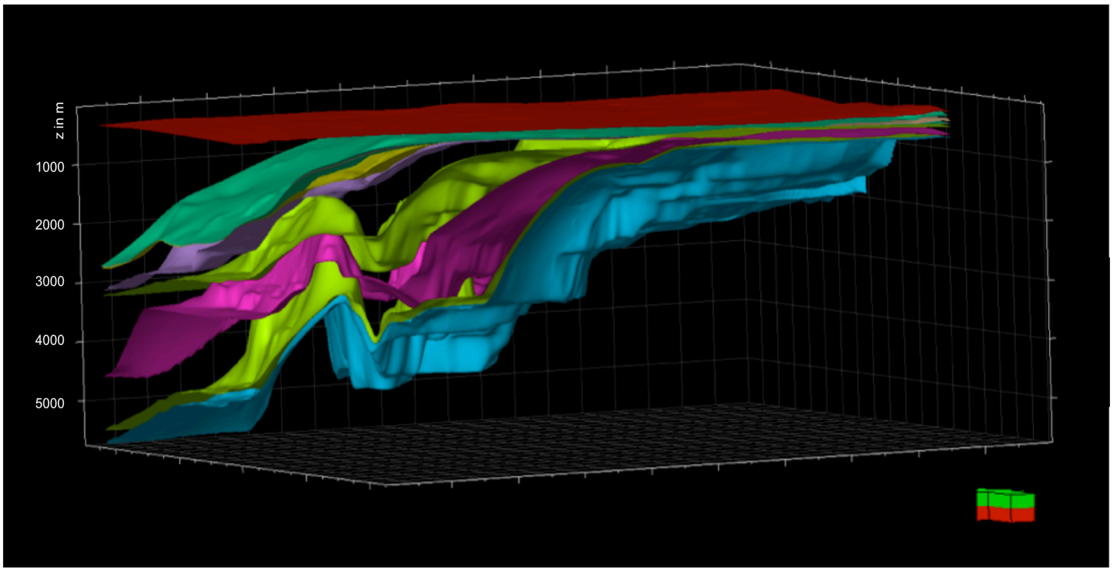

Figure 13. Model showing the 10 final depth maps from Seabed to Base Hekkingen on top of eachother (x:y:z=1:1:15).

8. Paleobathymetric Reconstruction

8.1 Methods

Paleobathymetry is defined as the study of water depths and topography of the sea floor and lakes in the geological past. It is an important, but often neglected parameter in basin analysis. Reconstruction of paleobathymetry is mainly accomplished according to two different approaches: (1) methods that are based on well data and (2) more profile/regional-based data. The main difference between these two is in scale and resolution. Studies based only on well data give a good temporal resolution but a low spatial resolution. They provide only information for single isolated points. In contrast, studies based on profile/regional-based data offer a good spatial but reduced temporal resolution due to the limitations of the seismic reflection data. In order to achieve the best result from the available data it can be necessary to combine both approaches.

In the following the different approaches for paleo-water depth reconstruction will be briefly explained.

8.1.1 Well-data based methods

Well-based water depth reconstruction is performed by the use of chemical, sedimentological and micropaleontological indicators of paleobathymetry from cores and cuttings.

Chemical bathymetric indicators

Chemical indicators are used in the paleobathymetric reconstruction based on the correlation between the chemical composition and/or trace element geochemistry of the sediments and the water depth (e.g. Ernst, 1970, Nicholls, 1967). Post-depositional diagenesis e.g. alteration, dissolution may modify the composition; hence this method should be used with care for older sediments.

In deep oceanic environments, the carbonate compensation depth (CCD) is the most important chemical indicator. Below the CCD, which is a dynamic boundary between 3000 and 5500 m (Barron & Whitman, 1981), calcium carbonate is absent in the sediments. Some mineral species, for example phosphates and glauconite may also provide indications for water depth (Allen & Allen, 1990).

Sedimentological bathymetric indicators

Sedimentary structures are useful as indicators for shallow marine and even more for continental environments. Coal, large hiatuses, and the absence of marine organisms and/or presence of terrestrial organisms are markers for continental environments. Shallow marine environments are often indicated by an increase of mud and bioturbation in comparison to near shore environments. The lower depth limit of the shallow marine environment is indicated by hummocky cross-stratification, a sedimentary structure which marks the storm wave base at a depth of about 200 m. In deep marine environments most of the sedimentary indicators do not provide satisfactory information to determine the paleo-water depth (Allen & Allen, 1990).

Micropaleontological bathymetric indicators

Micropaleontological indicators are probably the most widespread used method in paleo-water depth analysis. The method is based on the assumption that organisms living in the past shared a similar environment or depth range with present day analogues organisms (Gillmore *et al.,* 2001, Gradstein *et al.,* 1994).

The limitation of this method is that the older the sample is the number of species surviving into present day faunas becomes less. Furthermore, a change in the generic composition of faunas may also occur over time. Gillmore *et al*. (2001) presented an integrated approach based on the use of different faunal associations to determine maximum and minimum water depths for a given stratigraphic interval. Trace fossils may be used in addition to micropaleontological indicators.

8.1.2 Profile/Regional based methods

Tectonic modeling

In tectonic modeling the difference between the actual and the modeled subsidence curves are used to reconstruct the paleobathymetry (e.g. Lippard & Liu, 1992). The calculation of the modeled subsidence curve is usually based on the McKenzie (1978) rift model and does not take into account flexure, as it was performed in one dimension.

Flexural backstripping

Flexural backstripping is a post-rift basin restoration method, presented by Kusznir *et al.* (1991). The reconstruction of the basin is done in a stepwise manner taking into account thermal subsidence, derived from the McKenzie model (1978), flexural unloading and decompaction of the sediments. These three factors constrain the paleobathymetry, but faulting is not restored in this method. Roberts *et al.* (1998) highlighted the use of known paleobathymetric constraints, e.g. areas of zero or near zero paleo-water depth in the flexural backstripping method.

BP Backstripping

Another approach that is similar to the flexural backstripping was introduced by BP researchers (e.g. Young, 1992, Rattey & Hayward, 1993). In this reconstruction, the method of Kusznir *et al.* (1991) is combined with the restoration of faults. The first step is the removal of the overburden, followed by decompaction of the sediments, then the basement is unloaded and the thermal subsidence is restored. In the final step, faulting is restored using simple shear as deformation mechanism.

8.1.3 Paleobathymetry from depositional geometries

Kjennerud *et al*. (2001) introduced a structural restoration method where present depositional geometries from seismic sequences were used as the main input for a 2D reconstruction approach. Based on that, a 3D approach to palaobathymetric reconstruction was developed by Kjennerud & Sylta (2001) and implemented as a module in the hydrocarbon migration software SEMI. The paleobathymetry is reconstructed in 3D in a backwards manner starting with the present geometry. In order to estimate the paleobathymetry, the geometrical input from the seismic sequences and facies is combined with sedimententological and/or seismostratigraphic indicators of zero or near zero water depth and micropaleontological estimates. Decompaction is applied to each restored time step according to the decompaction curves of Sclater & Christie (1980).

Airy isostacy is taken into account, giving the possibility to correct for the isostatic response after decompaction. This method is used for the paleobathymetric reconstruction in this study and will be explained in more detail below.

8.2 Paleobathymetric Reconstruction with SEMI

8.2.1 Method

Two main approaches have been developed for the paleobathymetric reconstruction with depositional geometries according to two depositional scenarios (1) deep marine infill and (2) prograding sequences. During this reconstruction only the setting for deep marine infill was applied.

Deep marine infill:

Sediment units that onlap the basin flanks and show maximum thickness in the basin center contribute to the infilling of a relief created at an earlier stage. The deep marine infill approach is based on the correlation that maximum sediment thickness records the maximum bathymetry at a given time step.

During the reconstruction, the bathymetry of the base of the infilling unit is restored (Fig. 14). The first step is to flatten or shape the top of the infilling unit according to a known paleo-surface and then correct for Airy isostacy. Afterwards, the infilling unit is removed and the resulting relief gives a good picture of the paleo-relief at the base of the infilling unit. In the next step the defined calibration points for shallow or zero water depths are utilized to create a surface, which intersects all the defined emergent areas. Subtracting this surface from the relative relief restores the bathymetry (Kjennerud & Sylta, 2001).

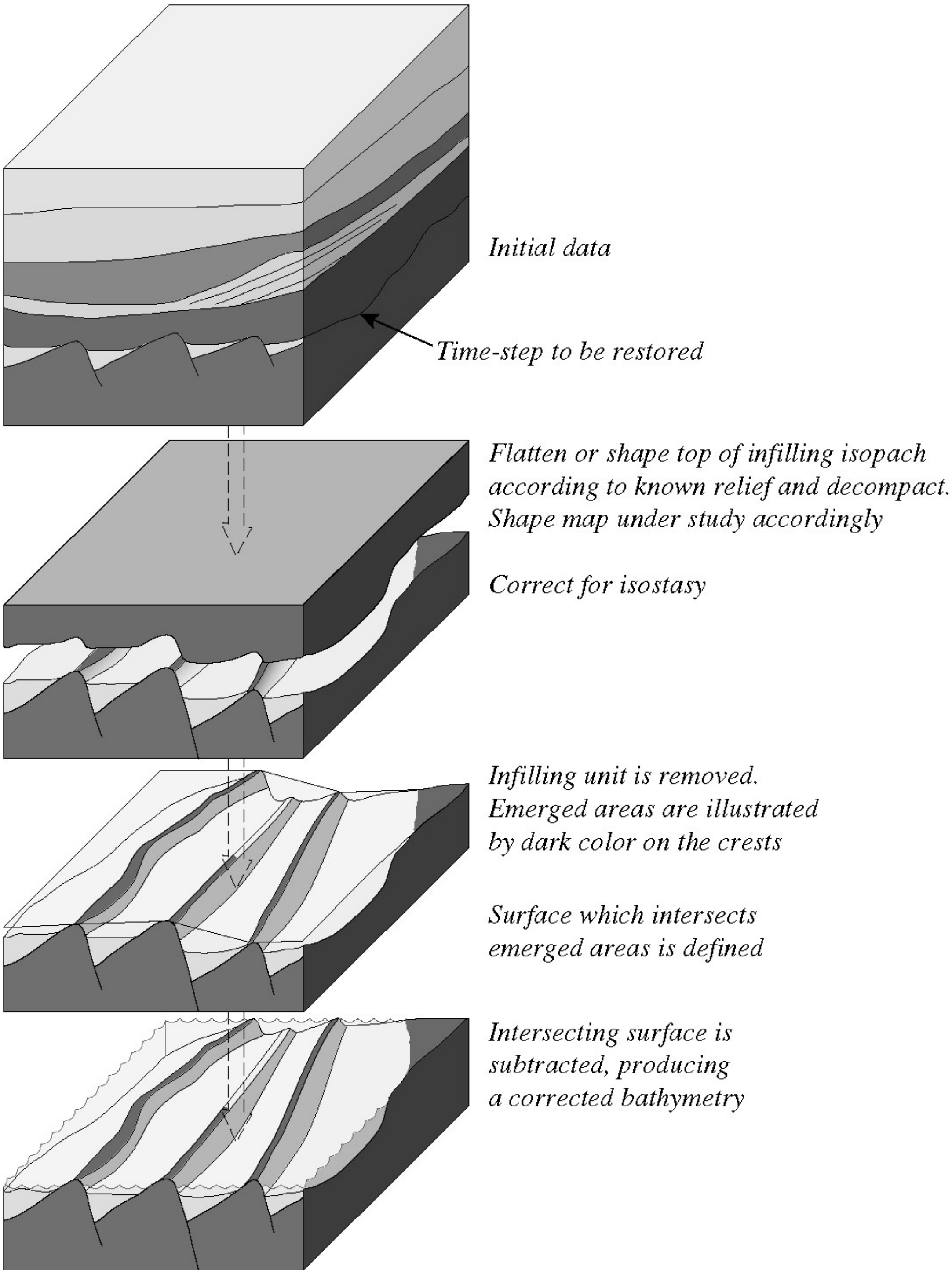

Figure 14. Method for restoring paleobathymetry in a deep marine infilling depositional scenario (modified after Kjennerud & Sylta, 2001).

8.2.2 SEMI workflow

The paleobathymetric reconstruction was accomplished employing SINTEF´s software SEMI Paleowater. The workflow is exemplified on the time step from 40 Ma to 66 Ma at 66 Ma, Base Torsk (Base Paleogene) and shown in Figures 15 a-g.

The reconstruction is conducted by calculating the accommodation space for the selected time step and subtracting the effects generated by other accommodation-creating processes. This is based on the idea that the accommodation space between two horizons is determined by decompaction and the water depth at the end of the deposition of this interval.

In the first step, the thickness between the selected surface and the one above is calculated and decompacted (Fig. 15 a). The decompaction is performed according to the porosity-depth relations of Sclater & Christie (1980), which was set up for dual lithology. Figure 16 shows the dual lithology setting used in the study described here.

In the next step, the Airy isostatic response to the decompacted thickness is calculated and subtracted from the previous calculated paleo-water depth (Fig. 15 b, c). Then the accommodation created by compaction of the underlying deposits is calculated and as well subtracted (Fig. 15 d, e). In the last step the water depth at end of deposition is added (Fig. 15 f). The resulting map describes the paleo-water depth formed by the pre-existing water depth and tectonic movements during the deposition of the selected time step. Afterwards this map is calibrated using geological data e.g. facies descriptions, well data and micropaleontological data from the literature (Fig. 15 g).

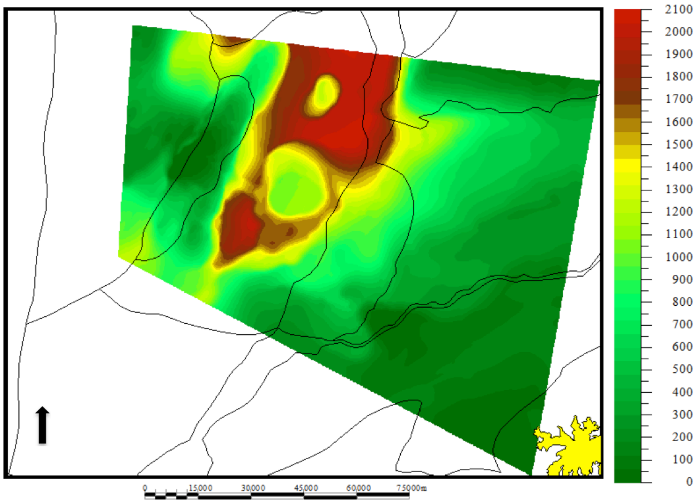

Figure 15 a. Decompacted thickness of the unit.

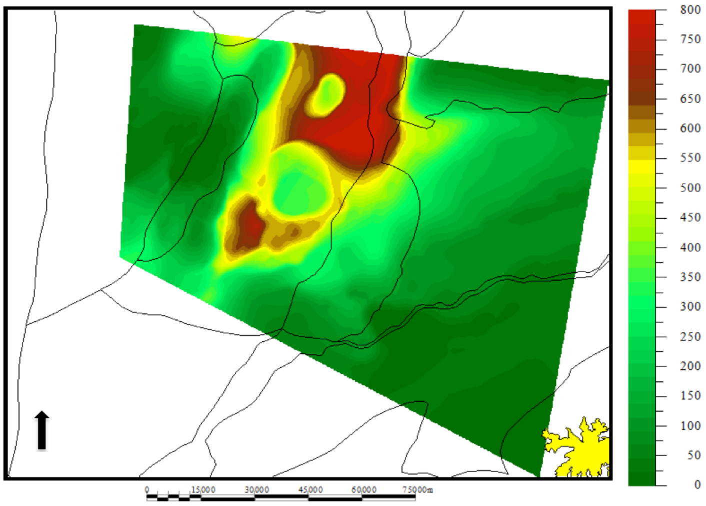

Figure 15 b. Amount of Airy isostatic response due to unloading of decompacted thickness.

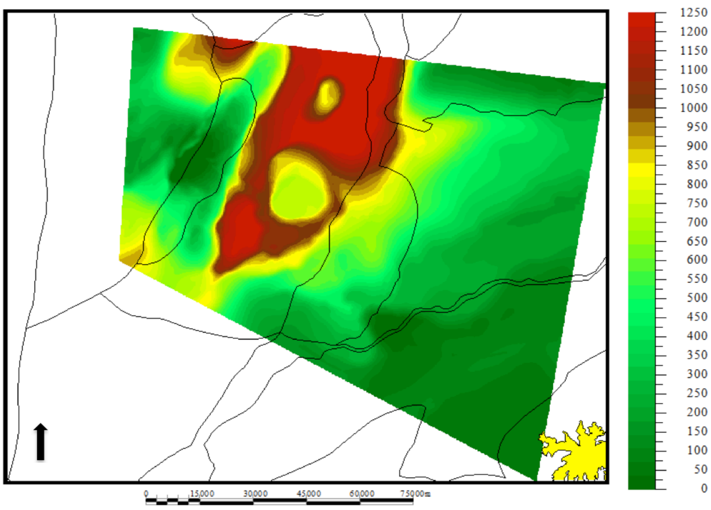

Figure 15 c. Correction for Airy isostasy.

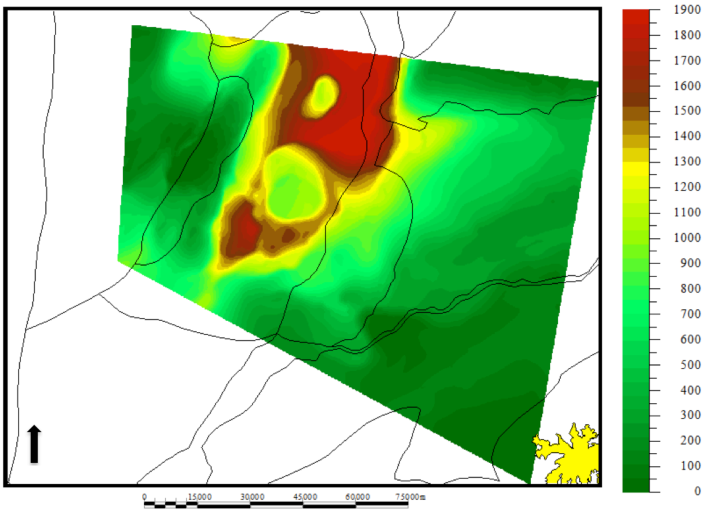

Figure 15 d. Amount of vertical changes due to compaction of underlying sediments.

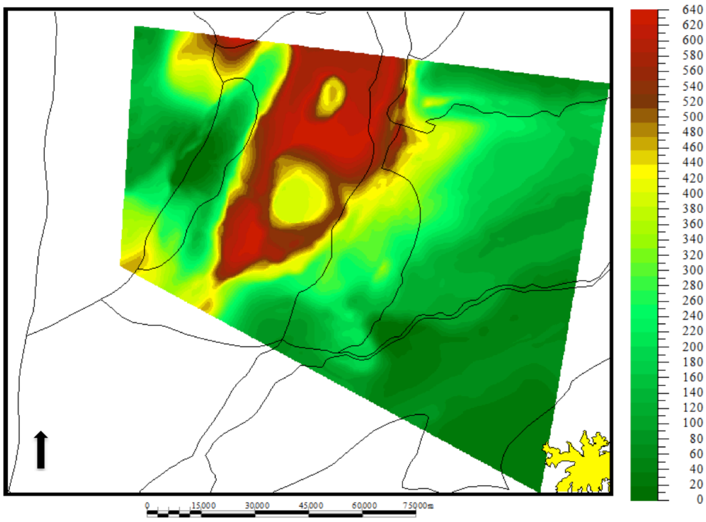

Figure 15 e. Correction for compaction below.

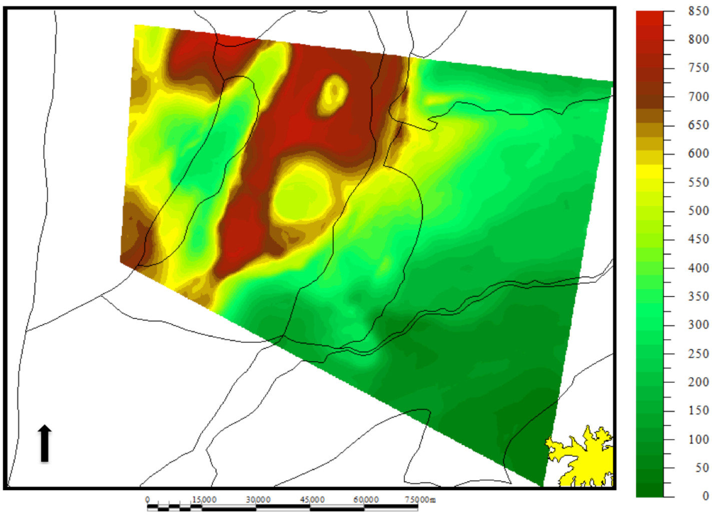

Figure 15 f. Resulting paleo-water depth after adding water depth from time step before.

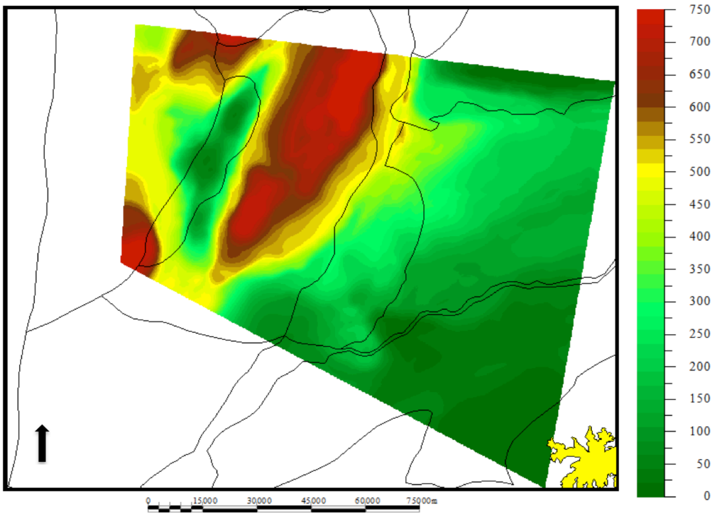

Figure 15 g. Final paleo-water depth map, corrected for salt dome artifacts and rifting.

Decompaction

	Name (optional)	Depositional Age		Lithology			Burial		
		From [Ma]	To [Ma]	#1	#2	Fraction #2	Waterdepth [m]	Depth [m]	Erosion [m]
1	Seabed - Base Pliocene	5	0	Shale	Sand	0.5		Seabed	
2	Base Pliocene - Intra Late Miocene	10	5	Shale	Silt	0.5		Intra_Sotbakken	
3	Intra Late Miocene - Base Miocene	23	10	Shale	Silt	0.5		Intra_Late_Miocene	
4	Base Miocene - Base Oligocene	34	23	Shale	Silt	0.2		Base_Miocene	
5	Base Oligocene - Middle Late Eocene	40	34	Shale	Sand	0.35		Base_Oligocene	
6	Middle Late Eocene - Base Palaeocene	66	40	Shale	Sand	0.2		Middle_Late_Eocene	
7	Base Palaeocene - Top Kolmule	100	66	Silt	Limestone	0.2		Base_Torsk	
8	Top Kolmule - Top Hekkingen	145	100	Shale	Silt	0.15		Kolmule	
9	Top Hekkingen - Base Hekkingen	156	145	Shale	Silt	0.1		Top_Hekkingen	
10	Base Hekkingen - Top Fuglen	158	156	Shale	Silt	0.5		Base_Hekkingen	

Figure 16. Input data for decompation modeling. Each row represents one time step. Lithology classification and fractions were taken from Inthorn *et al.* (2008).

8.3 Results

The paleo-water depth reconstruction was accomplished in this study from Base Hekkingen (Top Oxfordian) until the Intra Sotbakken/Base Pliocene in the area of the Hammerfest and Tromsø basins in the southwestern Barents Sea.

In total 9 time steps have been reconstructed using the software SEMI Paleowater and available information from literature e.g. sedimentological indicators of shallow or zero water depth and micropaleontological estimations. The previously generated depth maps from 2D seismic data have been used as an input.

The accuracy of the input data has to be taken into consideration while reconstructing the paleobathymetry. Especially in areas with sparse data distribution and outside of good well control, the generated depths maps used as input may rather reflect the interpolation method than the seismic interpretation. Another concern is the used velocity model during the depth conversion.

Since the reconstruction is done in a backwards manner starting with the present, structural features should be handled with care. Some of them might occur in older time steps as artifacts, even they have been formed later.

Another limitation of the modeling software is that tectonic processes e.g. rifting and thermal subsidence are not taken into account during the reconstruction modeling. Therefore this has to be taken into consideration manually after the preliminary restoration with SEMI.

In addition, the constraints used to calibrate the paleo-water depth restoration can add different uncertainties to the model. Constraints from zero water depths e.g. subaerial unconformities, absence of marine strata or coal add usually no uncertainty to the modeled water depths. Shallow marine indicators e.g. carbonate platforms have an uncertainty of around 20 m, which is still negligible in the paleobathymetric reconstruction. However, restoring deep marine areas can give larger uncertainties of up to several hundred meters (Kjennerud, 2001)

The following part describes the paleo-water depth reconstructions in relation with the ongoing geological development during that time.

All restorations are presented at the same depth scale, ranging from zero to 1000 m.

Base Hekkingen/Top Oxfordian (156 Ma)

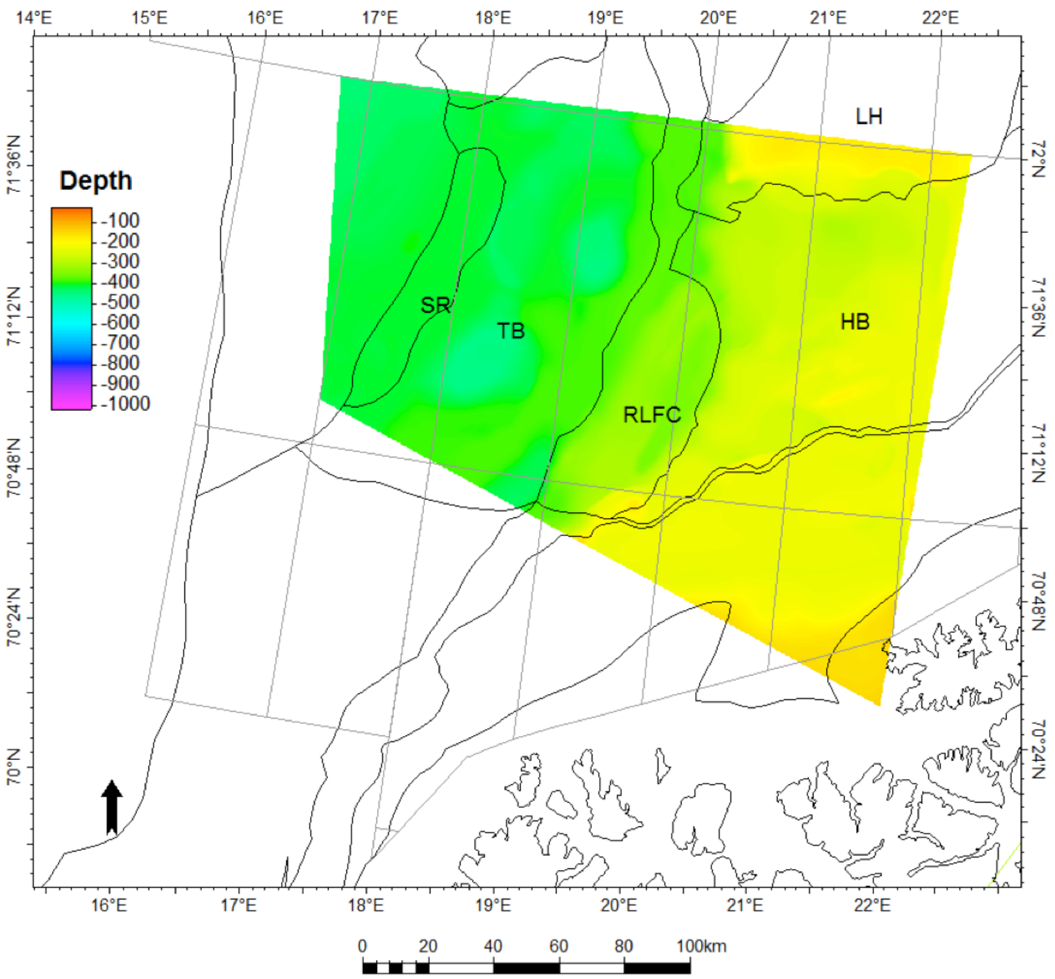

Figure 17. Paleo-water depth at Base Hekkingen/Top Oxfordian (145-156 Ma at 156 Ma).

A major sea level rise in Bathonian to Early Kimmeridgian cut off the supply of coarse clastics and resulted in the deposition of fine-grained sediments. Mainly shales and mudstones have been deposited in deep marine conditions. The dark shales are enriched in organic matter indicating a slow sedimentation rate without any current activity. Anoxic bottom water conditions characterize the depositional area that occurred because of Middle Jurassic tectonics causing block faulting and the formation of restricted basins

due to local barriers (Breivik *et al.,* 1998, Brekke *et al.*, 2001, Worsley *et al.,* 1988, Worsley, 2008). Due to the transgression, the highs were submerged. However, thickness variations in the deposited Hekkingen Formation between the Loppa High and the Hammerfest Basin indicate ongoing Jurassic tectonics (Worsley, 2008).
As described previously, the depth map for Base Hekkingen in the Tromsø and Sørvestsnaget basins had to be reconstructed due to sparse and noisy seismic data in the area at larger depths. The approach of using a relative thickness distribution between Base Torsk and Base Hekkingen led to thicknesses for the Hekkingen Formation of up to 700 m. However, according to the literature (NPD Factpages, Inthorn *et al.,* 2008) a thickness of less than 400 m can be assumed for the Hekkingen Formation. Therefore a new thickness map with variations from roughly 50 m to 300 m was constructed and added to the Top Hekkingen depth map to create a new Base Hekkingen depth map.

The preliminary reconstruction with SEMI showed water depths up to 1200 m in the deeper basins. The reconstruction was calibrated against the described deep marine restricted depositional environments (Henriksen *et al.,* 2011, Worsley, 2008). In addition, thickness information from the NPD Factpages and from Inthorn *et al.* (2008) have been taken into consideration.
The paleo-water depth map was multiplied by a factor of 0.6 to account for the tectonic subsidence. Thus, shallower water depths especially in the deep western basins have been obtained. Additionally, depths in the Hammerfest Basin, Tromsø Basin and Sørvestsnaget Basin have been decreased by 50 – 100 m, 100 m and 200 m, respectively. After the Loppa High showed too shallow areas, the paleo-water depths have been increased around 50 – 100 m on the structural high, taking into account that minor deposition of the Hekkingen Formation took place there as well.

The final paleo-water depth model shows water depths ranging from around 180 m on the Loppa High to 300 – 450 m in the deeper western basin areas (Fig. 17)

Top Hekkingen/Base Cretaceous (145 Ma)

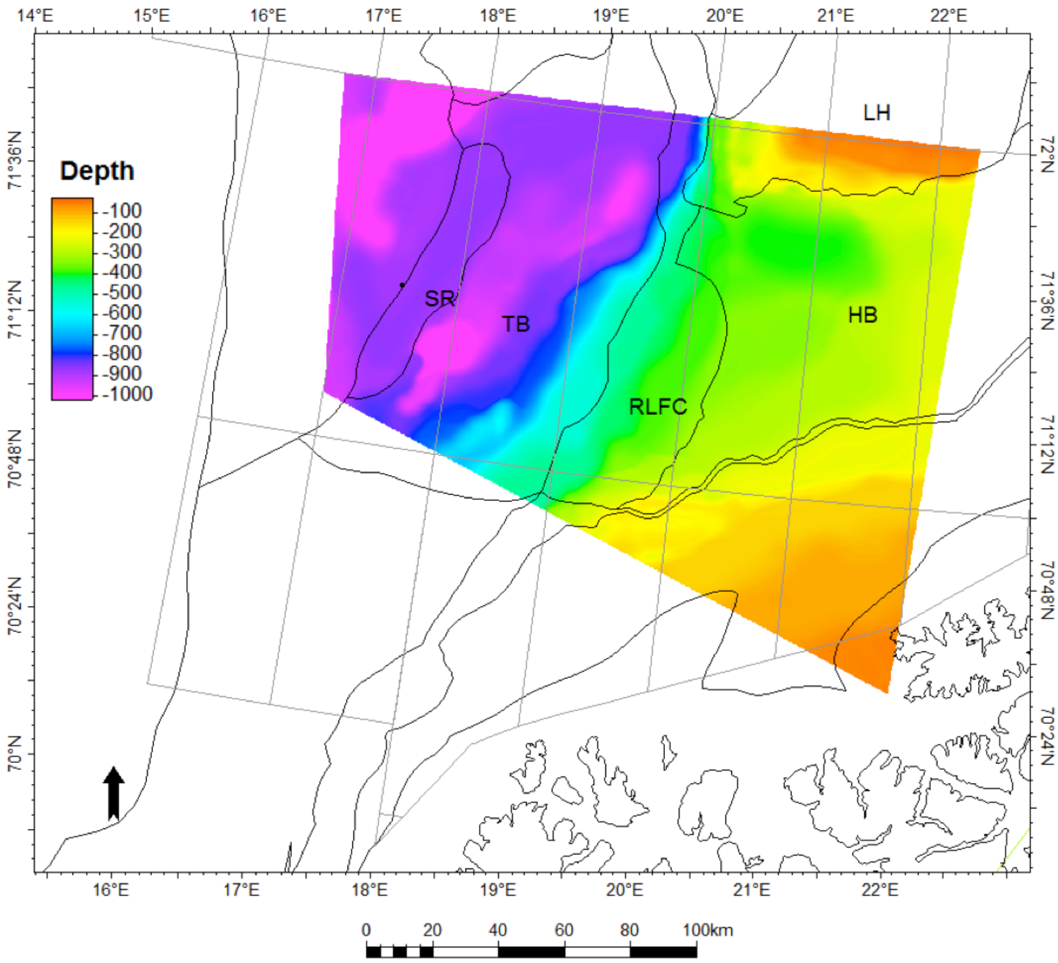

Figure 18. Paleo-water depth at Top Hekkingen/Base Cretaceous (100-145 Ma at 145 Ma).

At the transition from Late Jurassic – Early Cretaceous major rifting due to the break up of North Atlantic affected the whole area. Main tectonics occurred in the western Barents Sea, leading to wide rift basins, regional block-faulting and differential subsidence in the Hammerfest and Tromsø basins (Faleide *et al.,* 1993, Gabrielsen *et al.,* 1990).

In the deep marine basins like the Tromsø and Sørvestsnaget basins open marine mudstones and shales were accumulated. In the shallower Hammerfest Basin the mudstones were characterized by a lime-rich composition (Brekke *et al.,* 2001).

The rifting also led to uplift of the Loppa High, which continued to be a positive feature during most of the Cretaceous.

The initial reconstruction with SEMI showed basin depths in the western area of more than 2500 m and also up to 1000 m in the Hammerfest Basin. In comparison with older reconstructions (Inthorn *et al.,* 2008) this was assumed to be too deep. Additionally, bathymetric data of present day active rifting areas e.g. the Red Sea show that water depths along the active continental rift reach maximum depths of around 2000 m (e.g. Cochran, 2005). Therefore the whole map was multiplied with a factor of 0.6 in order to account for the tectonic subsidence during rifting. The Senja Ridge and the salt domes have been removed, because they form at later times and the areas in between have been interpolated with adjacent water depths. The depths in the Hammerfest, Tromsø and Sørvestsnaget basins have been decreased by another 200 m.

The resulting paleo-water depth map shows water depths in the Tromsø and Sørvestsnaget basins of around 700 - 1000 m, but local depocenters reach depths up to 1200 m (Fig. 18). Deep basins are developed because of the ongoing rifting process, which has its maximum at the Jurassic-Cretaceous boundary. The Hammerfest Basin shows depths between 200 - 500 m correlating with the shallower but still open marine environment supposed from the deposited sediments (Brekke *et al.*, 2001). On the Loppa High, depths around 50 m have been recorded. This is in agreement with the experienced uplift and the partial erosion along the high, confirmed by the observed sand bodies in the nearby Hammerfest Basin (Smelror *et al.,* 2009).

Top Kolmule/Cenomanian (100 Ma)

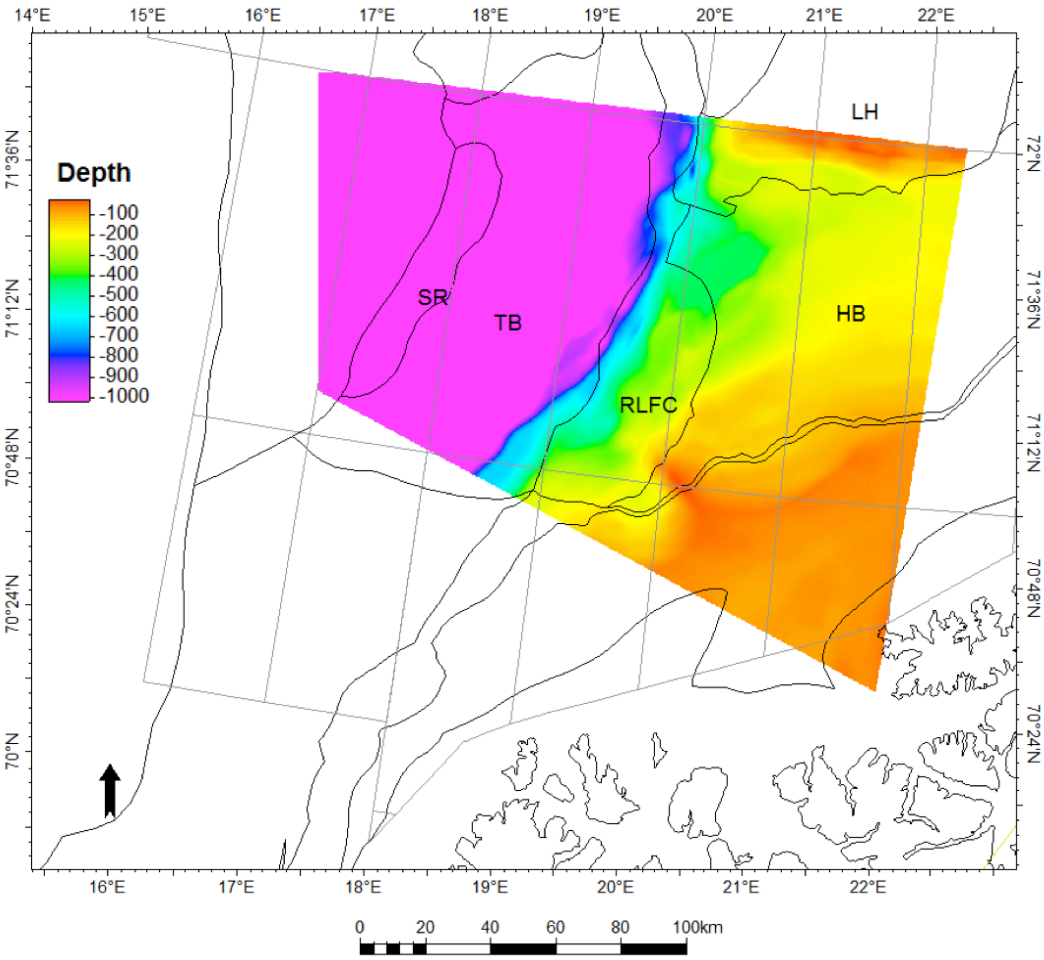

Figure 19. Paleo-water depth at Top Kolmule/Cenomanian (66-100 Ma at 100 Ma).

The sea level rise in Aptian/Albian times led to the deposition of a thick, deep marine shale sequence of the Kolmule Formation in the still subsiding basins. The Ringvassøy-Loppa Fault Complex separates the rapidly subsiding basins in the west from the more stable area towards the east (Faleide *et al.,* 1993). Thinner thickness of the Kolmule Formation in the Hammerfest Basin than in the western basins and sandy fans derived from the uplifted Loppa High support ongoing tectonics and the differential subsidence. This is also reflected in the paleo-water depth reconstruction showing shallower water depths in the Hammerfest Basin than in the Tromsø and Sorvestsnaget basins (Fig. 19).

By the end of Cenomanian the Kolmule Formation sediments covered most of the structural relief (Brekke *et al.,* 2001, Smelror *et al.,* 2009).

The sea level rise was followed by a renewed regression leading to the deposition of shales of the Kveite Formation in the deep basins and shallow marine carbonates and calcareous sandstones of the Kviting Formation in shallow basin areas and on platforms. Setoyama *et al.* (2011) analyzed foraminifera in wells in the Hammerfest and Tromsø basins and suggested more than 500 m water depth for the Kveite Formation in the Tromsø Basin. For the Kvitting Formation an outer shelf – upper bathyal environment with water depths between 100 and 500 m is assumed. This is in correlation with water depths shown in this conducted study, which range in the Hammerfest Basin between 150 and 500 m and are lower than 500 m and up to 1000 m for the western basins (Fig. 19).

The Senja Ridge has not been a structural high by that time, because uplift occurred later. Therefore the structural feature was cut out and the area was interpolated with adjacent water depths. The salt domes, which occur as an artifact in older maps, have been removed as well.

Base Torsk/Base Paleogene (66Ma)

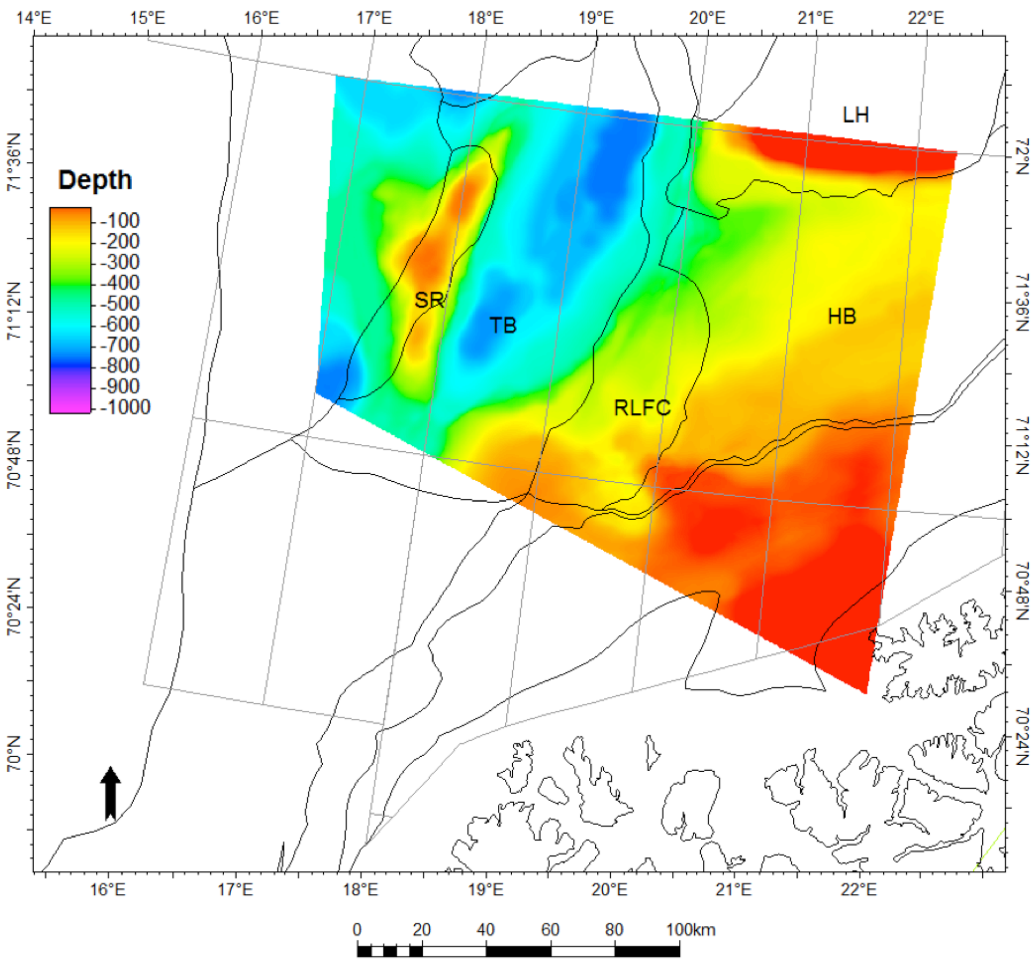

Figure 20. Paleo-water depth at Base Torsk/Base Paleogene (40-66 Ma at 66 Ma).

A pronounced hiatus occurred at the Cretaceous-Paleogene boundary in the western Barents Sea, where Late Paleocene mudrocks rest unconformably on Cretaceous strata in the Tromsø and Hammerfest basins. The analysis of micropaleontology in the upper Kviting Formation and the basal Torsk Formation in the Hammerfest Basin indicated similar deep marine environments during the deposition across the Late Cretaceous – Early Paleocene hiatus. This supported the suggestion that the possible presence of bottom currents might be a cause for the pronounced hiatus, together with uplift of the adjacent areas (Setoyama *et al.,* 2011).

Compressional tectonics in Late Cretaceous – Early Paleogene led to uplift of the Senja Ridge and on-lap of sandy mudrocks from the Sørvestsnaget Basin towards the Senja Ridge (Ryseth *et al.,* 2003). Tectonic activity also resulted in reactivation of the Asterias Fault Complex and the Loppa High continued to be a positive feature (Knutsen & Vorren, 1990). Throughout the Early Paleocene – Middle Eocene deposition of mudrocks took place in the Sørvestsnaget and Tromsø basins. Deposition of mudrocks in the Hammerfest Basin may be restricted to high sea level stands. In general shallower conditions occurred in the Hammerfest Basin than in the basins towards the west (Ryseth *et al.,* 2003, Smelror *et al.,* 2009).

The preliminary paleo-water depth reconstruction in SEMI gave depths up to more than 500 m in the Hammerfest Basin. The whole area was decreased in depth by multiplying with a factor of 0.85 and subtracting 80 m from the water depth, to account for tectonic subsidence. To take into account the uplift on the structural highs, the water depth was additionally decreased around 50 – 70 m on the Senja Ridge and around 50 m on the Loppa High. Furthermore, the salt domes in the Tromsø Basin have been removed and the area was interpolated with depths of surrounding areas. Main salt tectonics occurred in Early-Middle Eocene and has not yet been affecting the sea bottom during Early-Mid Paleocene (Ryseth *et al.,* 2003).

In the final model the water depths on the Senja Ridge and on the Loppa High range between 50 - 100 m and lower than 50 m, respectively (Fig. 20). This is in consistence with the observed silty and sandy deposits by Ryseth *et al.* (2003) in the nearby basins, indicating that the highs experienced erosion.
Deep marine conditions with water depths between 350 and 700 m occured in the Sørvestsnaget and Tromsø basins, leading to the deposition of mainly dark grey mudrocks (Ryseth *et al.,* 2003).

Top Torsk/Intra Late Eocene (40Ma)

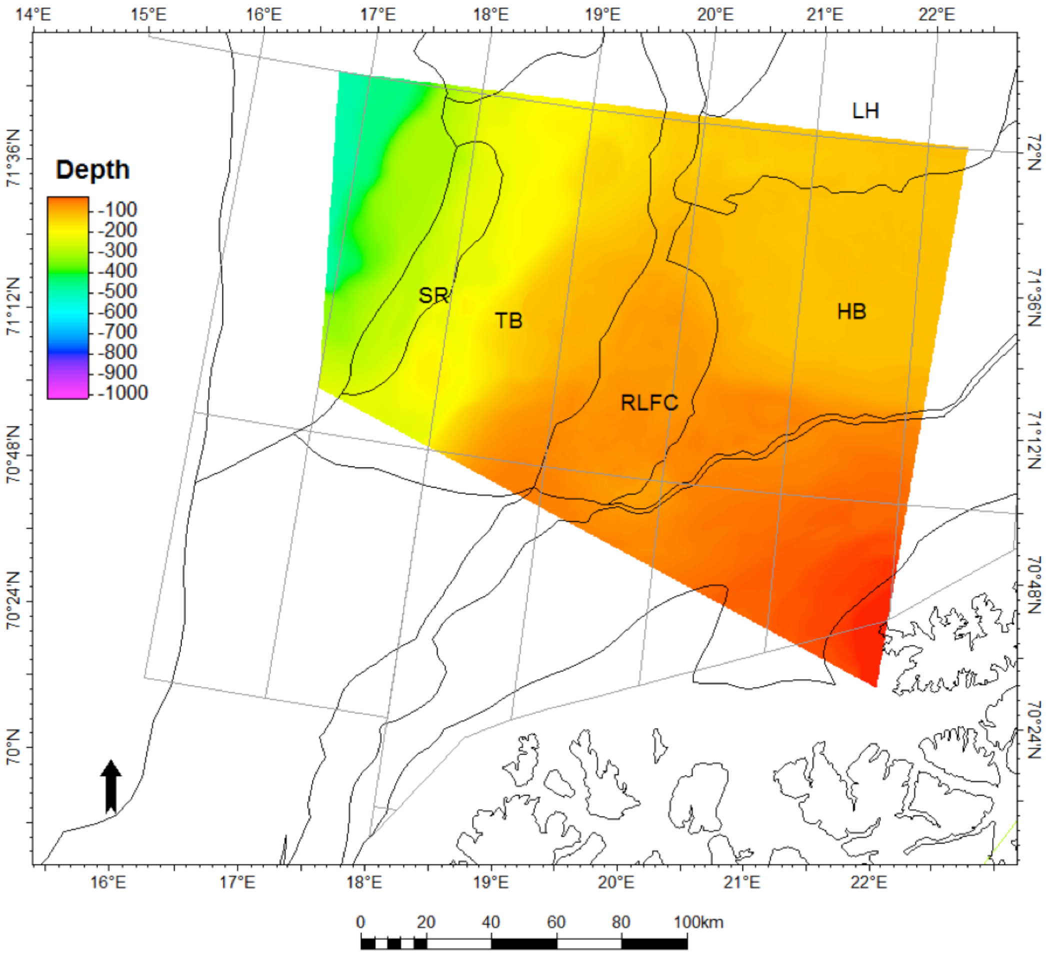

Figure 21. Paleo-water depth at Late Eocene (34-40 Ma at 40 Ma).

Deep marine conditions persisted in the Sørvestsnaget and Tromsø basins in Middle Eocene. In the Upper Eocene, a thin condensed layer was deposited, showing an equally deep marine environment as in the Middle Eocene, but with indications of the onset of a shallowing period towards the end of the Eocene (Fig. 21 - Fig. 23; Ryseth *et al.,* 2003).

In agreement with the condensed deep marine sedimentation, which occurred according to Ryseth *et al.* (2003) in the south Sørvestsnaget Basin, the paleo-water depth of the preliminary model was increased by 80 m in the whole area. Furthermore, it was multiplied by a factor of 0.85 to take into account the beginning of the shallowing.

The water depths of the final reconstruction are gradually deepening from around 100 m in the Hammerfest Basin up to 500 m in the Sørvestsnaget Basin (Fig. 21). The Loppa High and Senja Ridge are leveled out to adjacent marine areas of about 120 m and 250 m respectively.

Base Oligocene (34 Ma)

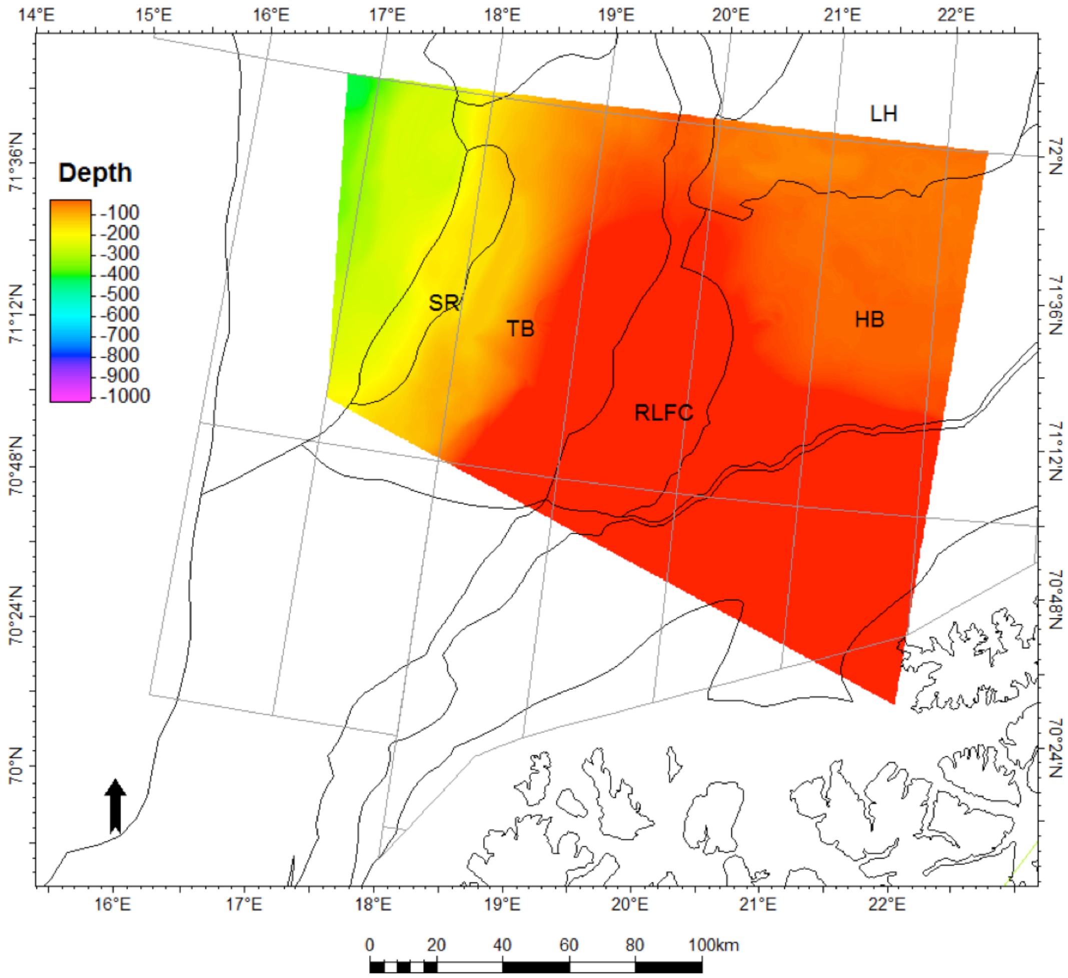

Figure 22. Paleo-water depth at Base Oligocene (23-34 Ma at 34 Ma).

After the period of deep marine conditions in Early-Mid Eocene, a significant shallowing occurred throughout the region in Late Eocene – Early Oligocene. This might be related to the Early Oligocene reorganization of spreading poles (Faleide *et al.,* 1993). In general, during Oligocene the margin became tectonically quiet and shallow marine conditions occurred throughout the whole Oligocene-Miocene with condensed sedimentation and phases of local erosion (Fig. 22 – Fig. 24).

The initial paleo-water depth reconstruction with SEMI was calibrated against the depositional environment description of the sediments in wells in the Sørvestsnaget Basin and on the Senja Ridge according to Ryseth *et al.* (2003). Water depths have been decreased around 40 m and the area was multiplied by a factor of 0.9 to account for the period of shallowing caused by the reorganization of spreading poles.

In the final reconstruction, water depths range between above sea level and 350 m. Water depths on the Loppa High, Hammerfest Basin and Ringvassøy-Loppa Fault Complex are lower than 50 m (Fig. 22). Sediments in the Sørvestsnaget Basin are mainly dominated by fine-grained mudrocks, and the reconstruction shows water depths around 200 to 350 m. On the eastern side of the Senja Ridge, a thin unit of glauconitic sandstone was deposited indicating accumulation in a more nearshore setting, with water depths lower than 150 m in the Tromsø Basin (Ryseth *et al.,* 2003).

Base Miocene (23Ma)

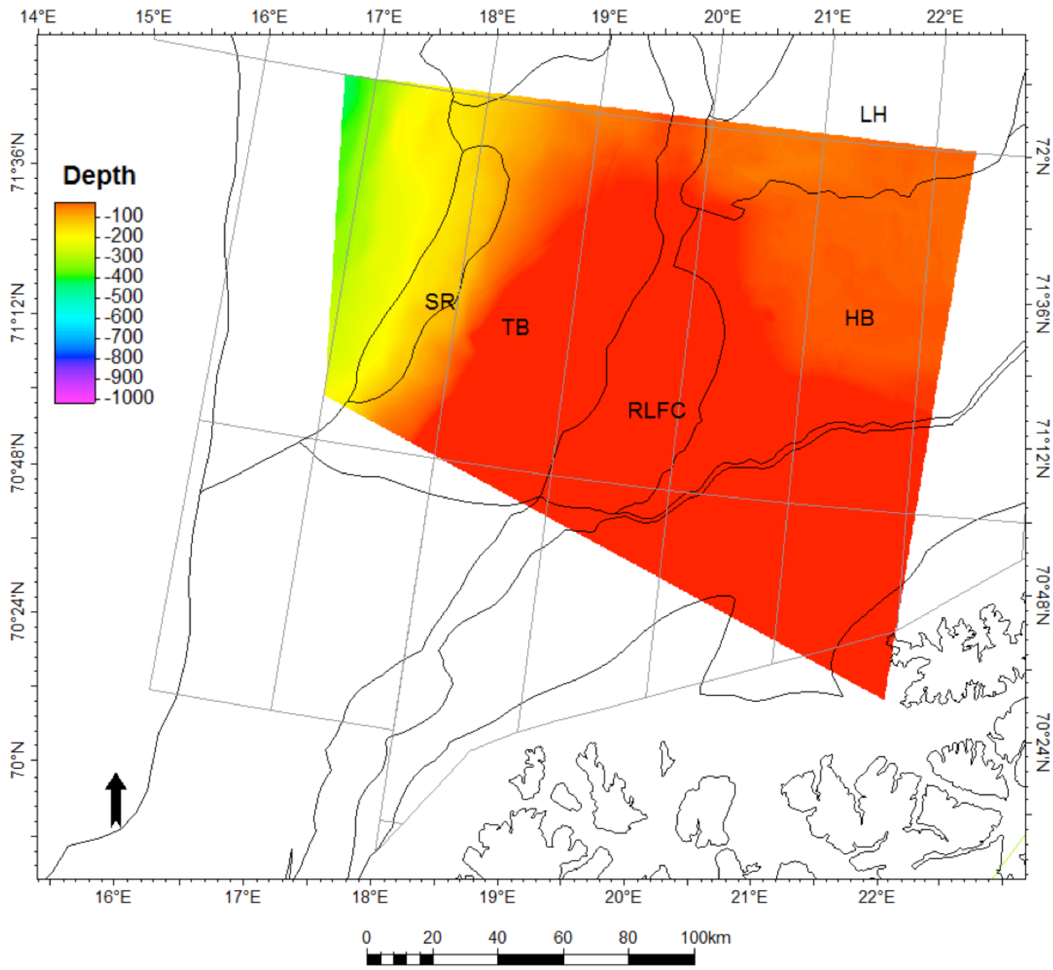

Figure 23. Paleo-water depth at Base Miocene (10-23 Ma at 23 Ma).

The boundary of Miocene-Oligocene is characterized by a pronounced break in sedimentation of about 13 Ma. In the Sørvestsnaget Basin, the whole succession from Chattian (Late Oligocene) until Serrevalian (Late-Middle Miocene) is missing. Sediments from Middle-Upper Miocene in the Sørvestsnaget Basin comprise silty mudrocks with sandstone layers (Ryseth *et al.,* 2003). The depositional environment continues to be shallow marine.

The initial paleo-water depth map was decreased by 50 m and multiplied with a factor of 0.9. This takes into account the since Oligocene ongoing period of low tectonic activity and shallowing.

In the final reconstruction depths around 200 – 350 m have been recorded in the Sørvestsnaget Basin. The Hammerfest and Tromsø basins show water depths below 50 m. Areas on the Ringvassøy-Loppa Fault Complex and closer to the Finnmark Platform have been even emergent, reflecting erosion or non-deposition during this time (Fig. 23).

Intra Upper Miocene (10 Ma)

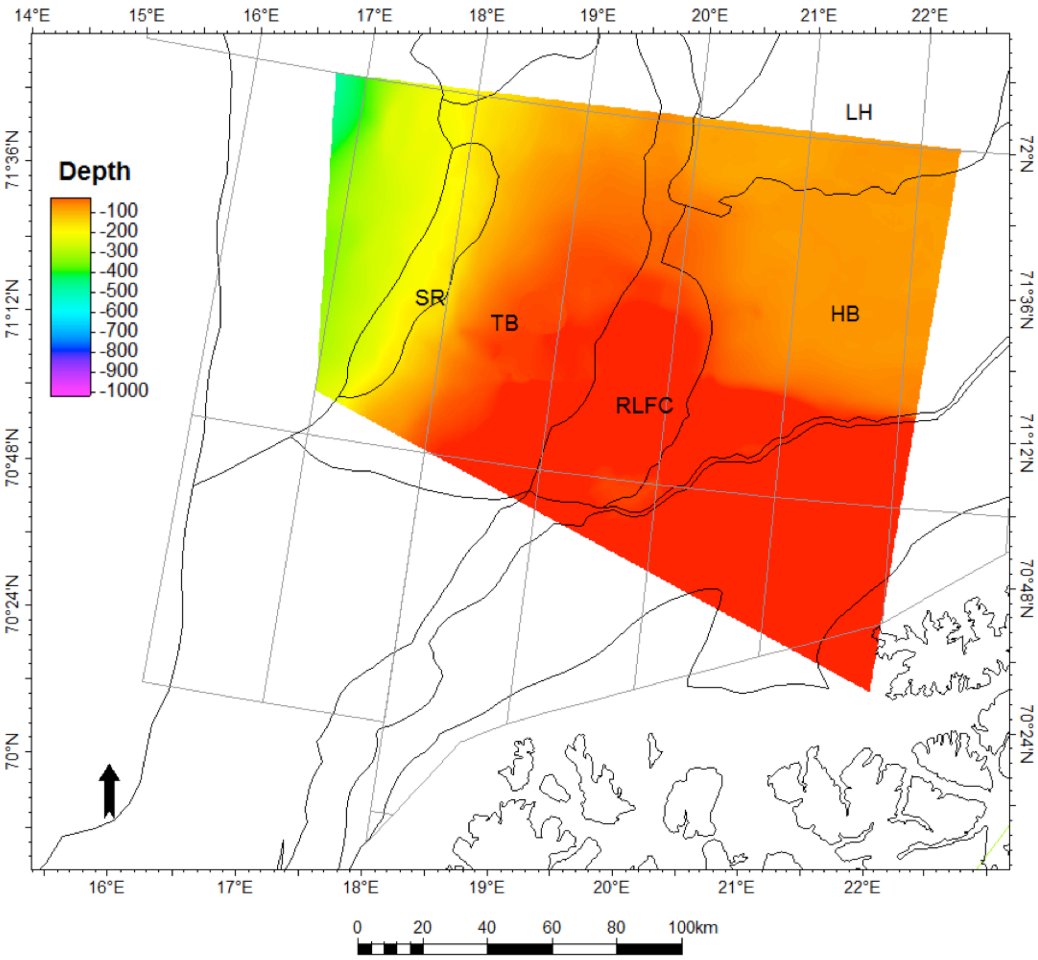

Figure 24. Paleo-water depth for Intra Upper Miocene (5-10 Ma at 10 Ma).

The shift of active rifting further north and the transition of the active western margin towards a passive one since the Oligocene led subsequently to thermal subsidence along the passive margin generating accumulation space for a thick Neogene sedimentary wedge in the western Barents Sea (Fig. 22 - Fig. 25). This is coincident with the uplift and widespread erosion of the eastern Barents Sea and Svalbard (Brekke *et al.,* 2001, Ryseth *et al.,* 2003). The Late Miocene is still characterized by shallow marine conditions passing into deeper environments towards the west (Ryseth *et al.,* 2003).

The preliminary reconstructed model with SEMI has been decreased by 70 m and multiplied by a factor of 0.85. This gave an acceptable result taking into account on the one side the persisting shallow marine conditions and on the other side the thermal subsidence (Fig. 24).

In the final model, the Hammerfest Basin shows depths below 50 m with emergent areas closer to the Finnmark Platform. Up to 150 m have been recorded in the Tromsø Basin. The deepest area occurs in the west nearer to the passive margin, where depths up to 500 m were reached.

Intra Sotbakken/Base Pliocene (5 Ma)

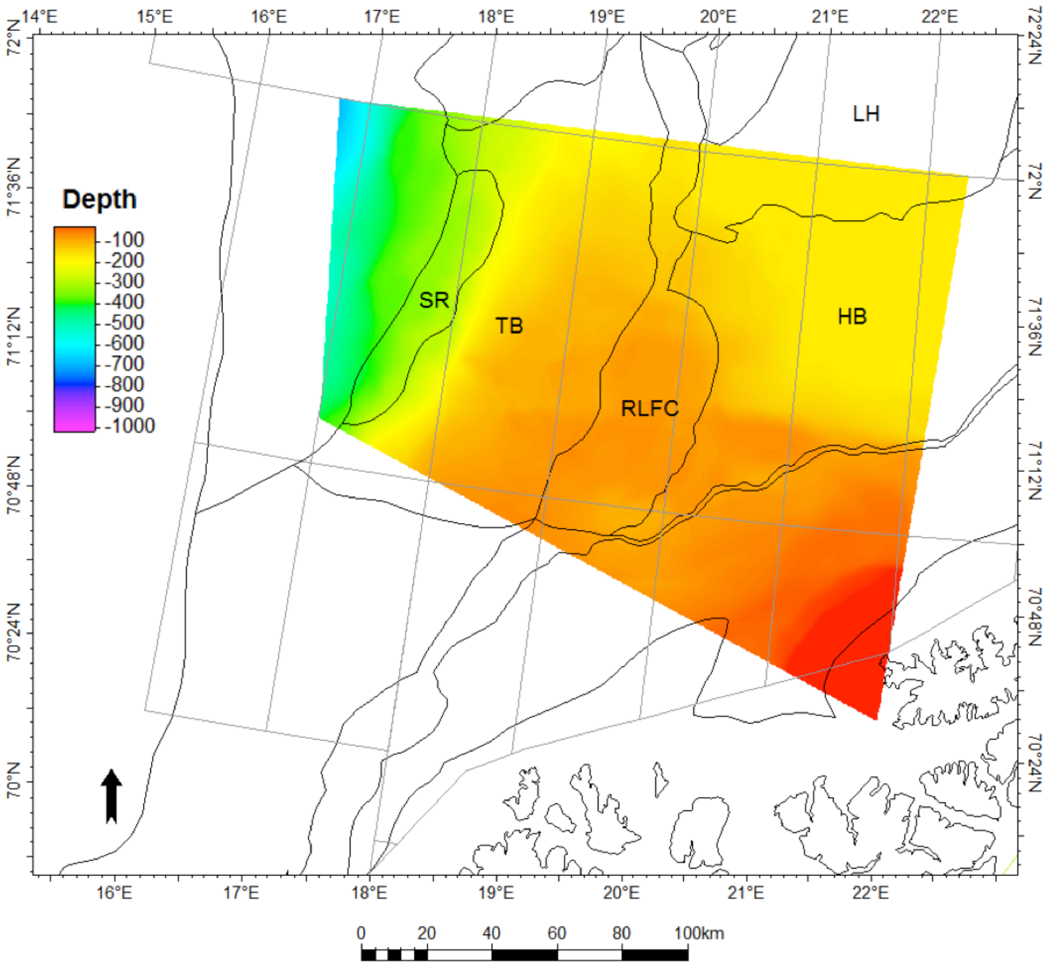

Figure 25. Paleo-water depth for Base Pliocene (0-5 Ma at 5 Ma).

The Paleocene-Miocene succession is truncated by an Upper Pliocene-Pleistocene glacial sedimentary wedge, which thickens towards the west. The clinoforms are related to progradation of glacial deltas supplied by eroded material from the uplifted shelf to the east (Dahlgreen *et al.,* 2005, Faleide *et* *al.,* 1996, Ryseth *et al.,* 2003) The Neogene to recent regional uplift and erosion is estimated to be around 0 - 1000 m in the Tromsø Basin, 700 - 1000 m in the Hammerfest Basin, and 1000 - 1500 m on the Loppa High. The severity of the exhumation may have caused leakage from former hydrocarbon accumulations (Cavanagh *et al.,* 2006).

In order to take into account the uplift and the described glacial marine environment in the east of the study area, the water depths of the preliminary reconstruction were decreased by 150 m.

Depths in the final reconstruction range between less than 100 to 650 m. The deepest depths can be found in the Sørvestsnaget Basin, increasing from around 400 to 650 m (Fig. 25). The Hammerfest Basin shows depths around 150 - 200 m, decreasing to less than 100 m in the Ringvassøy-Loppa Fault Complex, the Tromsø Basin and close to the Finnmark Platform.

9. Comparison with Integrated Barents Sea study - BMU 2008

SINTEF Petroleum Research conducted the Integrated Barents Sea study – Basin Modelling Upgrade (Inthorn *et al.,* 2008) over the southern Norwegian Barents Sea in 2008. Part of the project was the paleobathymetric reconstruction. The study area in 2008 incorporated a larger area including the Stappen High and Bjarmeland Platform in the north, the Nordkapp Basin and Finnmark Platform in the east and reached until the western margin. The reconstruction was done from intra – Late Permian (Wuchiapingian) to the Base Quarternary and included in total 18 time steps. The time steps from Base Hekkingen until Present have been the same like in the here performed study, but in Inthorn *et al.* (2008) two additional time steps have been accomplished between Top Hekkingen and Base Cenomanian and one more time step at Base Quaternary.

Differences in the results between the two studies result not only from dissimilarities in the size of the study area and amount of reconstructed time steps, but also because of better data coverage in Inthorn *et al.* (2008). This led to different seismic interpretations and hence different depth maps as input in the reconstruction process.

A smaller area of interest in this project led to the question if this will result in a more precise paleo-water depth reconstruction due to the fact that the calibration with data from the literature can be done on a smaller scale. However, the sparse seismic input data in this study limited the possible effect because of less detailed interpretation. In the following part the differences between the present study and Inthorn *et al.* (2008) are described for each time step.

Top Oxfordian (145-156 Ma at 156 Ma)

The comparison of the models from 2008 and 2012 show similar settings in the Hammerfest Basin with minor shallower conditions of around 10 – 40 m in the model from 2008. Larger differences occur across the Ringvassøy-Loppa Fault Complex, where the reconstruction from 2012 records depths around

300 - 370 m and the model from 2008 shows shallower conditions with depths of roughly 230 – 300 m.

Base Cretaceous (100-145 Ma at 145 Ma)

The model from 2012 generally shows deeper conditions of 30 - 120 m in the Hammerfest Basin and 50 - 150 in the Tromsø and Sørvestsnaget basins. Some of the differences may arise because two additional time steps have been modeled in 2008 between the time steps 100 and 145 Ma. In addition, minor geometrical differences occur for the location of the depocenters in the basins. The reconstruction from 2012 records a depocenter in the southern part of the Tromsø Basin, whereas in the model from 2008 a depocenter is located in the north of the basin. However, both show depths increasing up to 1200 m. Minor differences also arise on the Loppa High, where around 20 - 50 m shallower water depths exist in the recent model.

Base Cenomanian (60-100 Ma at 100 Ma)

The comparison in this time step shows similar depths for both models in the Hammerfest Basin and the Loppa High. However, the areas of the Tromsø and Sørvestsnaget basins show large differences in depths and geometry. In general, the reconstruction from 2008 is characterized by deeper conditions. Both models show a depocenter in the central Tromsø Basin with depths around 1200 – 1300 in the model from 2012 and depths around 1500 - 1800 m from 2008. Furthermore, a second depocenter occurs in the northern part of the model from 2008, which is lacking in the one from 2012. Additionally, the model from 2008 is characterized by two positive structures at the border from the Tromsø to the Sørvestsnaget Basin, showing water depths between 200 - 300m. These do not exist in the recent reconstruction, possibly due to sparser data coverage. Another dissimilarity is the large difference in depth in the Sørvestsnaget Basin, where depths of up to 1800 m are recorded in the older model, whereas depths around 1000 - 1200 m, similar to the Tromsø Basin, occur in the model from 2012. The similar depths as in the Tromsø Basin in model 2012 can be explained because in this study it is assumed, that a pronounced subsidence affecting the Sørvestsnaget Basin more than the Tromsø Basin occurred in the end of Late Cretaceous.

Base Paleogene (40-60 Ma at 60 Ma)

Several differences are found between the model from 2008 and 2012, but in general, the geometries are similar and both reconstructions show that the Loppa High and the Senja Ridge existed as positive features during that time. The paleo-water reconstruction from 2012 shows around 50 – 150 m deeper conditions in the western Hammerfest Basin, the Ringvassøy-Loppa Fault Complex and the Tromsø Basin. In 2008, the model included several small salt domes in the Tromsø Basin. Similar structures in the model from 2012 have been removed due to the explanation that the salt movement occurred later. Another difference appears in the depocenters in the Sørvestsnaget Basin where depths between 500 - 750 m occur in the model from 2012 while depths of 700 – 1300 m are reached in the deepest parts in the reconstruction of 2008. This implies a steeper gradient for the Sørvestsnaget Basin and a larger subsidence of the basin assumed in the model from 2008.

Intra Late Eocene (34-40 Ma at 40 Ma)

A comparison of the reconstructed paleobathymetry in the northwestern Hammerfest Basin and the Loppa High shows around 50 - 80 m shallower water depths in the model from 2012. Furthermore, the model in 2012 shows a smooth deepening towards the west, beginning in the central Tromsø Basin with depths around 100 - 150 m and increasing down to 400 – 500 m in the western end of the study area. In the reconstruction from 2008, the water depths start at around 100 m further west on the Senja Ridge deepening down to 350 - 400 m in the Sørvestsnaget Basin. This indicates a steeper gradient from the land area to outer shelf areas in the model from 2008.

Base Oligocene (23-34 Ma at 34 Ma)

The differences between the two models in this time step comprise up to 50 m deeper conditions on the Loppa High, Hammerfest Basin and eastern Tromsø Basin in the model from 2012. Furthermore, it shows that deepening towards the west begins in the central Tromsø Basin and depths increase gradually from 150 m up to 400 m on the western border of the study area. However, the model from 2008 shows that the deepening begins only on the west of the Senja Ridge with depths around 50 m increasing up to 250 m in the Sørvestsnaget Basin. This implies that about 100 - 200 m more accumulation space for sediments from the east existed in the Sørvestsnaget Basin in the model from 2012.

Base Miocene (10-23 Ma at 23 Ma)

The comparison shows similar depths and geometries for both models in the Loppa High, the Hammerfest Basin and the Tromsø Basin. However, the model from 2008 shows a more rapid transition from inner to outer shelf areas. Deepening begins on the western edge of the Senja Ridge with depths around 50 – 100 m increasing down to 400 m in the Sørvestsnaget Basin. In the model from 2012, the deepening begins in the western Tromsø Basin and the Senja Ridge is characterized by depths around 150 m, increasing in the Sørvestsnaget Basin to similar depths as in the model from 2008.

Intra Late Miocene (5-10 Ma at 10 Ma)

The overall geometries in the 2008 and 2012 models are similar, but better seismic data coverage indicates that the depth model from 2008 is more detailed than the 2012 model. Additionally, Loppa High, Hammerfest Basin and Senja Ridge are deeper by about 20 - 50 m, 20 - 70 m and 20 - 150 m, respectively. The area of the Ringvassøy-Loppa Fault Complex and the southern Tromsø Basin also show deeper conditions in the model from 2012, where depths slightly below sea level occur. In the reconstruction from 2008, 20 – 150 m shallower water depths are recorded and hence the areas are partially emergent.

Base Pliocene (0-5 Ma at 5 Ma)

A comparison of the paleo-water depth model from 2008 and 2012 shows slightly deeper conditions of about 30 - 70 m in the Loppa High and the northeastern Hammerfest Basin. Both maps show a deepening towards the west, but the 2012 model shows a more rapid deepening. Here, the change from inner to outer shelf areas begins immediately east of the Senja Ridge showing depths of 250 – 350 m, while depths of 300 – 500 m are seen in the Sørvestsnaget Basin. The 2008 model recorded depths between 150 - 200 m for the Senja Ridge while depths around 200 - 250 m persist in the Sørvestsnaget Basin, deepening to 400 m at the western edge of the study area.

10. Conclusion

This thesis accomplished a paleo-water depth reconstruction in the southwestern Barents Sea in the area of the Hammerfest and Tromsø basins.
Before the actual reconstruction process time and depth maps have been produced from seismic interpretation. In total six horizons from Seabed to Base Hekkingen have been interpreted on 13 seismic lines covering the area. Additionally, major fault interpretation has been conducted. Well top data of 28 wells located in the study area have been used as support for the interpretation. Six time maps have been generated from the interpreted horizons and were used together with the faults as an input to build a Geomodel. In order to receive depth maps a velocity model was formed and the Geomodel has been depth converted. Four additional horizons inbetween Base Pliocene and Base Torsk have been constructed to fill in the model.
The final edited depth maps represented the input data for the paleobathymetric reconstruction. In total 9 time steps from Base Hekkingen/Top Oxfordian to Intra Sotbakken/Base Pliocenes have been accomplished in this study. The reconstruction was performed using SINTEF´s software SEMI Paleowater, based on a modified deep marine infill approach described by Kjennerud (2001).
The modeled paleo-water depth maps have been calibrated e.g. with sedimentological and microplaeontolgical data from the literature.
The reconstruction of the paleo-water depth showed the following trends:

- During deposition of the Hekkingen Formation a restricted deep marine environment characterized the area with depths around 180-450 m.
- Late Jurassic-Early Cretaceous rifting led to subsidence of the basins and deep marine conditions persisted. At the same time, the Loppa High developed as a positive feature. Differential subsidence between rapidly subsiding western basins and a more stable area in the east continued during the Cretaceous.
- Opening of the Norwegian-Greenland Sea led to compressional tectonic and the uplift of the Senja Ridge and Loppa High in Early Paleogene.

- A significant phase of shallowing took place at Late Eocene – Early Oligocene, which may be related to a reorganization of spreading poles. Shallow marine conditions persisted throughout Oligocene-Miocene.
- Transition to a passive continental margin and development of oceanic crust since the Oligocene led to subsidence along the margin and deposition of a thick Neogene sedimentary wedge, comprising sediments derived from a glacial – bathyal environment. This was coincident with widespread uplift and erosion of the eastern Barents shelf.

The comparison to the accomplished IBS-BMU 2008 showed several smaller differences resulting mainly from different input data. Especially the sparse seismic data coverage in this study had a great influence on the details of the reconstructed structures.

For further work, denser data coverage is suggested and more time steps should be conducted to get an improved paleobathymetric reconstruction.

The results from the paleo-water depth restoration are an important input in further basin modeling work e.g. in burial history reconstruction and hydrocarbon migration modeling.

References

Allen,P. & Allen, J.R., 1990. Basin Analysis Principles & Applications. Blackwell Science. 451 pp.

Barrère, C., Ebbing, J., Gernigon, L., 2011. 3-D density and magnetic crustal characterization of the southwestern Barents Shelf: implications for the offshore prolongation of the Norwegian Caledonides. Geophysical Journal International, Vol. 184, 1147-1166.

Barron, E.J. & Whitman, J.M., 1981. Oceanic sediments in space and time. In: Emiliani, C. (Ed.), The Sea, Wiley Interscience, New York, Vol. 7, 689-733.

Brekke, H., Sjulstad, H.I., Magnus, C., Williams, R.W., 2001. Sedimentary environments offshore Norway – an overview. In: Martinsen, O.J., Dreyer, T. (Eds.), Sedimentary environments offshore Norway – Palaeozoic to Recent. Norwegian Petroleum Society (NPF), Amsterdam, Elsevier, Special Publication Vol. 10, 7-37.

Breivik, A.J., Gudlaugsson, S.T., Faleide, J.I., 1995. Ottar-Basin, SW Barents Sea - a major Upper Paleozoic rift basin containing large volumes of deeply buried salt. Basin Research, Vol. 7, 299-312.

Breivik, A.J., Faleide, J.I., Gudlaugsson, S.T., 1998. Southwestern Barents Sea margin: late Mesozoic sedimentary basins and crustal extension. Tectonophysics, Vol. 293, 21-44.

Cavanagh, A.J., di Primio, R., Scheck-Wenderoth, M., Horsfiled, B., 2006. Severity and timing of Cenozoic exhumation in the southwestern Barents Sea. Journal of the Geological Society, London, Vol. 163, 761-774.

Cochran, J. R., 2005. Northern Red Sea: Nucleation of an oceanic spreading center within a continental rift. Geochem. Geophys. Geosyst.,Vol. 6.

Dahlgreen, K.I.T., Vorren, T.O., Stoker, M.S., Nielsen, T., Nygård, A., Sejrup, H.P., 2005. Late Cenozoic prograding wedges on the NW European continental margin: their formation and relationship to tectonics and climate. Marine and Petroleum Geology Vol. 22, 1089-1110.

Dengo, C.A. & Røssland, K.G., 1992. Extensional tectonic history of the western Barents Sea. In: Larsen, R., Brekke, H., Larsen, B. and Talleraas, E. (Eds.), Structural and tectonic modelling and its application to petroleum geology. Elsevier, Amsterdam, 91-107.

Ernst, W.,1970. Geochemical Facies Analysis. Amsterdam, Elsevier, 152 pp.

Faleide, J.I., Gudlaugsson, S.T., Jacquart, G., 1984. Evolution of the western Barents Sea. Marine and Petroleum Geology, Vol. 1, 123-150.

Faleide, J.I., Vågnes, E., Gudlaugsson, S.T., 1993. Late Mesozoic-Cenozoic evolution of the south-western Barents Sea in a regional rift-shear tectonic setting. Marine and Petroleum Geology, Vol. 10,186-214.

Faleide, J.I., Solheim, A., Fiedler, A., Hjelstuen, B.O., Andersen, E.S., Vanneste, K., 1996. Late Cenozoic evolution of the western Barents Sea-Svalbard continental margin. Global and Planetary Change, Vol. 12, 53-74.

Faleide, J.I. and Petrobar Team, 2009. Crustal architecture and basin evolution in the Barents Sea. Geophysical Research Abstracts, Vol. 11, EGU 2009-12236.

Henriksen, E., Ryseth, A.E., Larssen, G.B., Heide, T., Rønning, K., Sollid, K., Stoupakova, A.V., 2011. Chapter 10, Tectonostratigraphy of the greater Barents Sea: implications for petroleum systems. In: Spencer et al. (Eds.), Arctic Petroleum Geology.Geological Society London, Memoirs, Vol. 35, 163-195.

Gabrielsen, R.H., Færseth, R.B., Jensen, L.N., Kalheim, J.E. and Riis, F., 1990. Structural elements of the Norwegian continental shelf, Part I: The Barents Sea Region. Norwegian Petroleum Directorate Bulletin, Vol. 6, 47 pp.

Gabrielsen, R.H., Grunnaleite, I., Rasmussen, E., 1997. Cretaceous and Tertiary inversion in the Bjørnøyrenna Fault Complex, south-western Barents Sea. Mar. Pet. Geol. Vol. 14 (2), 165-178.

Gillmore, G.K., Kjennerud, T., Kyrkjebø, R., 2001. The reconstruction and analysis of paleowater depth: a new approach and test of micropaleontological approaches in the post-rift (Cretaceous to Quaternary) interval of the Northern North Sea. In: Martinsen, O. and Dreyer, T. (Eds.), Sedimentary Environments Offshore Norway – Paleozoic to Recent. Norwegian Petroleum Society Special Publication, Vol. 10, 365-379.

Glørstad-Clark, E., Faleide, J.I., Lundschien, B.A., Nystuen, J.P., 2010. Triassic seismic sequence stratigraphy and paleogeography of the western Barents Sea Area. Marine and Petroleum Geology, Vol. 27, 1448-1475.

Gradstein, F.M., Kaminski, M.A., Berggren, W.A., Kristiansen, I.L., D´Iorio, M., 1994. Cenozoic biostratigraphy of the North Sea and Labrador Sea. Micropaleontology, Vol. 40, 152 pp.

Gudlaugsson, S.T., Faleide, J.I., Johansen, S.E., Breivik, A.J., 1998. Late Palaeozoic structural development of the South-western Barents Sea. Marine and Petroleum Geology, Vol. 15, 73-102.

Inthorn, M., Daszinnies, M.C., Felix, M., Hvoslef, S., Mann, U., Nielsen, J.K., Ritter, U., Weiss, H.M., 2008. Integrated Barents Sea Study - Basin Modelling Upgrade 2008, SINTEF Petroleum Research Report 24.6759.00/01/08. Confidential.

Johansen, S.E., Gudlaugsson, S.T., Svånå, T.A., Faleide, J.I., 1994. Late Paleozoic evolution of the Loppa High, Barents Sea. Unpublished PhD thesis, University of Oslo, Oslo, 25 pp.

Kjennerud, T. ,2001. Paleobathymetry and rift basin evolution. With particular reference to the northern North Sea. PhD Thesis, Norwegian University of Technology and Science.

Kjennerud, T. & Sylta, Ø., 2001. Application of quantitative paleobathymtry in basin modelling, with reference to the northern North Sea. Petroleum Geoscience Vol. 7(4), 331-341.

Knutsen, S.M. & Vorren, T.O., 1991. Early Cenozoic sedimentation in the Hammerfest Basin. In: T.O. Vorren, H. Sejrup and J. Thiede (Eds.), Cenozoic Geology of the Northwest European Continental Margin and Adjacent Deep Sea Areas. Mar. Geol., Vol. 101, 31-48.

Kusznir, N.J., Marsden, G., Egan, S.S., 1991. A flexural cantilever simple-shear/pure-shear model of continental lithosphere extension: application to the Jeanne d´Arc Basin, Grand Banks and Viking Graben, North Sea. In: Roberts, A.M., Yelding, G., Freeman, B. (Eds.), The Geometry of Normal Faults. Geological Society of London, Special Publication, Vol. 55, 207-228.

Larssen, G.B., Elvebakk, G., Henriksen, L.B., Kristensen, S.E., Nilson, I., Samuelsberg, T.J., Svånå, T.A., Stemmerik, L., Worsley, D., 2005. Upper Paleozoic lithostratigraphy of the southern part of the Norwegian Barents Sea. Norges Geologiske Undersøkelse Bulletin, Vol. 444, 3-43.

Lippard, S.& Liu, G., 1992. Tectonic modelling of the northern North Sea using program RIFT. In: Larsen et al. (Eds.), Structural and Tetconic Modelling and its Application to Petroleum Geology. NPF Special Publication Vol. 1, 43-54.

Mc Kenzie, D.P., 1978. Some remarks on the development of sedimentary basins, Earth and Planetary Science Letters, Vol. 40, 25-32.

Mørk, A., Dallmann, W.K., Dypvik, H., Johannessen, E.P., Larssen, G.B., Nagy, J., Nøttvedt,A., Olaussen, S., Pechelina, T.M., Worsley, D., 1999. Mesozoic lithostratigraphy. In: Dallmann, W.K. (Ed.), Lithostratigraphic lexicon of Svalbard. Review and recommendations for nomenclature use. Upper Paleozoic to Quarternary bedrock. Norsk Polarinstitutt, Tromsø, 127-214.

Nicholls, G.D., 1967. Trace elements in sediments: an assessment of their possible utility as depth indicators. Marine Geology, Vol. 5, 439-555.

Nøttvedt, A., Cecchi, M., Gjelberg, J.G., Kristensen, S.E., Lønøy, A., Rasmussen, A., Rasmussen, E., Skott, P.H., van Veen, P.M., 1992. Svalbard-Barents Sea correlation: a short review. In: Vorren, T.O., Bergsager, E., Dahl-Stamnes, Ø.A., Holter, E., Johansen, B., Lie, E., Lund, T.B. (Eds.), Arctic Geology and Petroleum Potential, Amsterdam (Elsevier). NPF Special Publication Vol. 2, 363-375.

Ohm, S. E., Karlsen, D. E., Austin, T. J. F., 2008. Geochemically driven exploration models in uplifted areas: examples from the Norwegian Barents Sea. American Association of Petroleum Geologists Bulletin, 92, 1191–1223.

Rattey, R.P. & Hayward, A.B., 1993. Sequence stratigraphy of a failed rift system: the Middle Jurassic to Early Cretaceous basin evolution of the Central and Northern North Sea. In: Parker, J. R. (Ed.), Petroleum Geology of Northwest Europe: Proceedings of the 4th Conference. Geological Society, London, 215-249.

Roberts, A.M., Kusznir, N.J., Yielding, G., Styles, P., 1998. 2D flexural backstripping of extensional basins: the need for a sideways glance. Petroleum Geoscience, Vol. 4, 327-338.

Ryseth A., Augustson J.H., Charnock M., Haugerud O., Knutsen S.-M., Midbøe P.S., Opsal J.G. & Sundsbø G., 2003. Cenozoic stratigraphy and evolution of the Sørvestsnaget Basin, southwestern Barents Sea. Norwegian Journal of Geology, Vol. 83, 107-128.

Samuelsberg, T., Elvebakk, G., Stemmerik, L., 2003. Late Paleozoic evolution of the Finnmark Platform, southern Norwegian Barents Sea. Norwegian Journal of Geology, Vol. 83, 351-362.

Sclater, J.G. & Christie, P.A.F., 1980. Continental stretching: an explanation of the post-mid Cretaceous subsidence of the central North Sea basins. Journal of Geophysical Research, Vol. 85, 3711-3739.

Setoyama, E., Kaminski, M.A., Tyszka, J., 2011. The Late Cretaceous-Early Paleocene paleobythymetric trends in the southwestern Barents Sea – Palaeoenvironmental implication of benthic foraminiferal assemblage analysis. Paleogeography,Paleoclimatology, Paleoeocology, Vol. 307 (1-4), 44-58.

Sheriff, R.E. & Geldart, L.P., 1995. Exploration Seismology, Cambridge University Press, 628 pp.

Smallwood, J.R., 2002. Use of V_0-K depth conversion from shelf to deep-water: how deep is that brightspot? First break, Vol. 20, 99-107.

Smelror, M., Petrov O.V., Larssen, B.B., Werner, S., 2009. Atlas Geological History of the Barents Sea. Geological Survey of Norway, Trondheim.

Stemmerik. L. & Worsley, D., 2005. 30 years on – Arctic Upper Paleozoic stratigraphy depositional evolution and hydrocarbon prospectivity. Norwegian Journal of Geology, Vol. 85, 151-168.

Vail, P.R., Mitchum, R.M., Todd, R.G., Widmeier, J.M., Thompson, S., Sangree, J.B., Bubb, J.N., Hatlelid, W.G., 1977. Seismic stratigraphy and global changes of sea level. In: Payton, C.V. (Ed.), Seismic Stratigraphy – Applications to Hydrocarbon Exploration. American Association of Petroleum Geologists Memoir, Vol. 26, 49-212.

Veeken, P.C.H, 2007. Handbook of Geophysical Exploration – Seismic Stratigraphy, Basin Analysis and Reservoir Characterization, Elsevier, Vol. 37.

Wood, R.J., Edrich, S.P., Hutchison, I., 1989. Influence of North Atlantic tectonics on the large-scale uplift of the Stappen High and Loppa High, western Barents Shelf. In: Tankard, A.J. and Balkwill, H.R. (Eds.), Extensional Tectonics and Stratigraphy of the North Atlantic Margins. American Association of Petroleum Geologists, Memoir, Vol. 46, 559-566.

Worsley, D., 2008. The post-Caledonian geological development of Svalbard and the Barents Sea. Norsk Geologisk Forening. Abstracts and Proceedings, Vol. 3, 5-21.

Worsley, D., Johansen, R., Kristensen, S.E., 1988. The Mesozoic and Cenozoic succession of Tromsøflaket. In: Dalland, A., Worsley, D., Ofstad, K. (Eds.), A lithostratigraphic scheme of the Mesozoic and Cenozoic succession offshore Mid- and Northern Norway. Norwegian Petroleum Directorate (NPD) Bulletin 4, 42-65.

Young, R., 1992. Restoration of a regional profile across the Magnus Field in the northern North Sea. In: Larsen et al. (Eds.), Structural and Tectonic Modelling and its Application to Petroleum Geology, Norwegian Petroleum Society Special Publication, 221-229.

Ziegler, P.A., 1978. North-Western Europe: tectonics and basin development, in: Key-notes of the MEGS II (Amsterdam, 1978) Geol. Mijnbouw, Vol. 57, 589-626.

www.npd.no , factpages (29.05.2012)

Appendix

Index to Appendix

Table of Figures:

Final Depth maps:

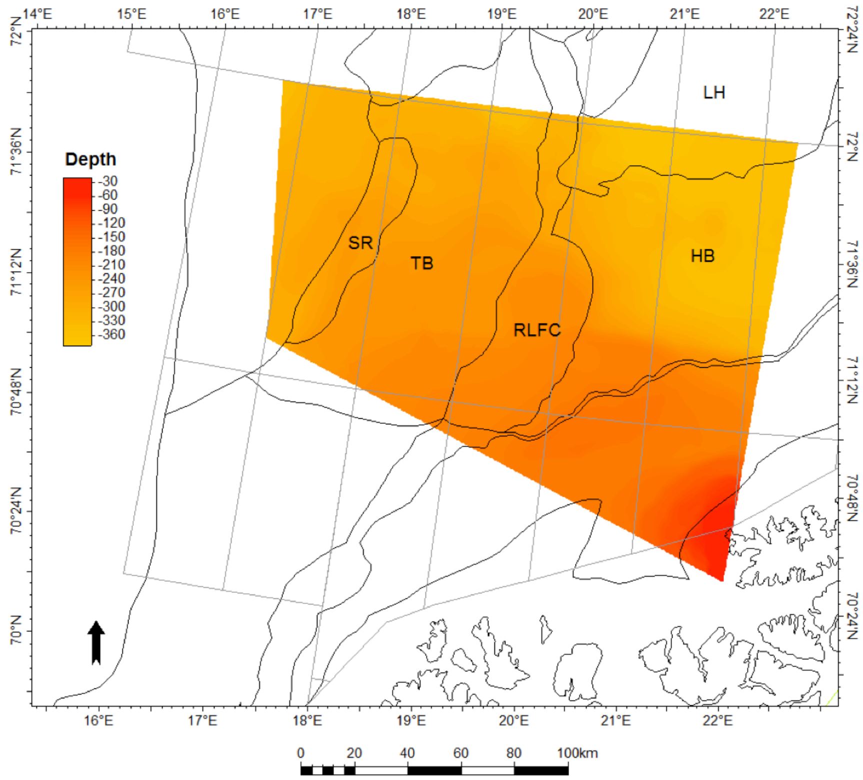

Figure 1. Depth map Seabed.

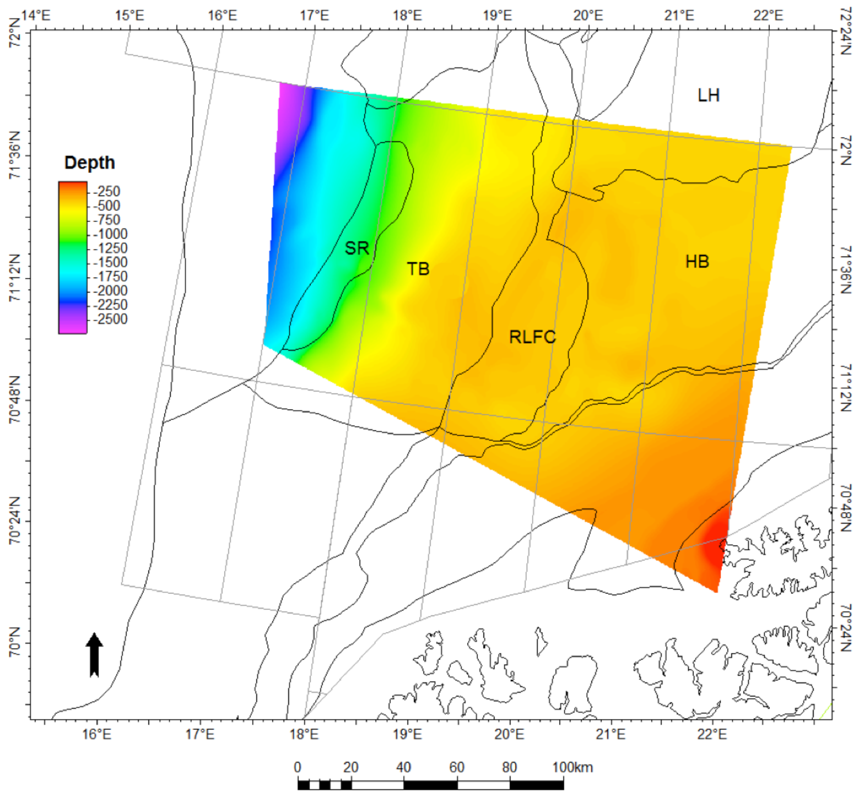

Figure 2. Depth map Intra Sotbakken.

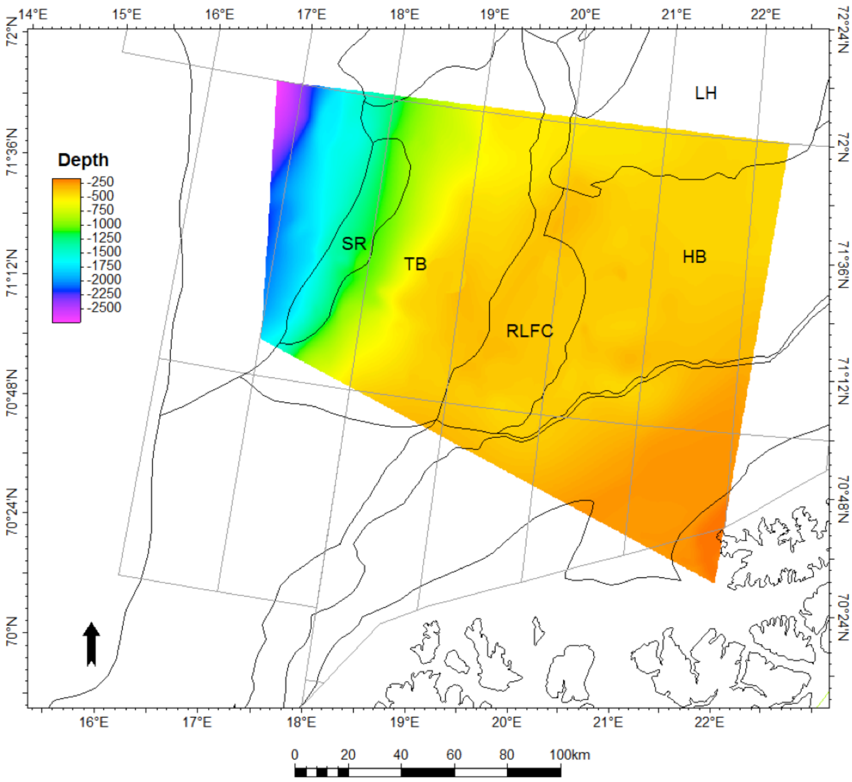

Figure 3. Depth map Intra Upper Miocene.

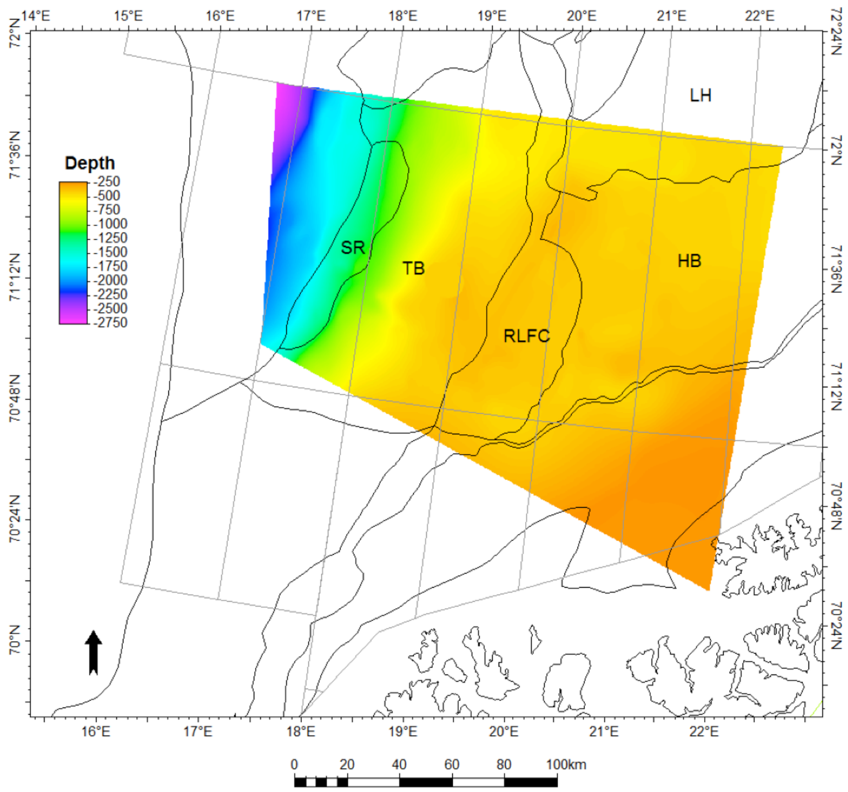

Figure 4. Depth map Base Miocene.

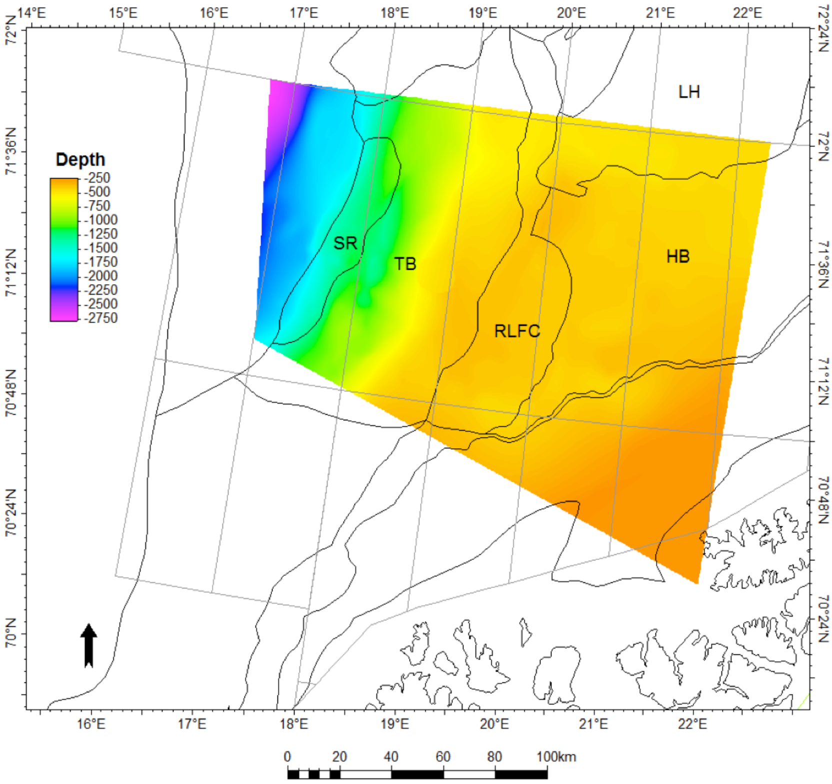

Figure 5. Depth map Base Oligocene.

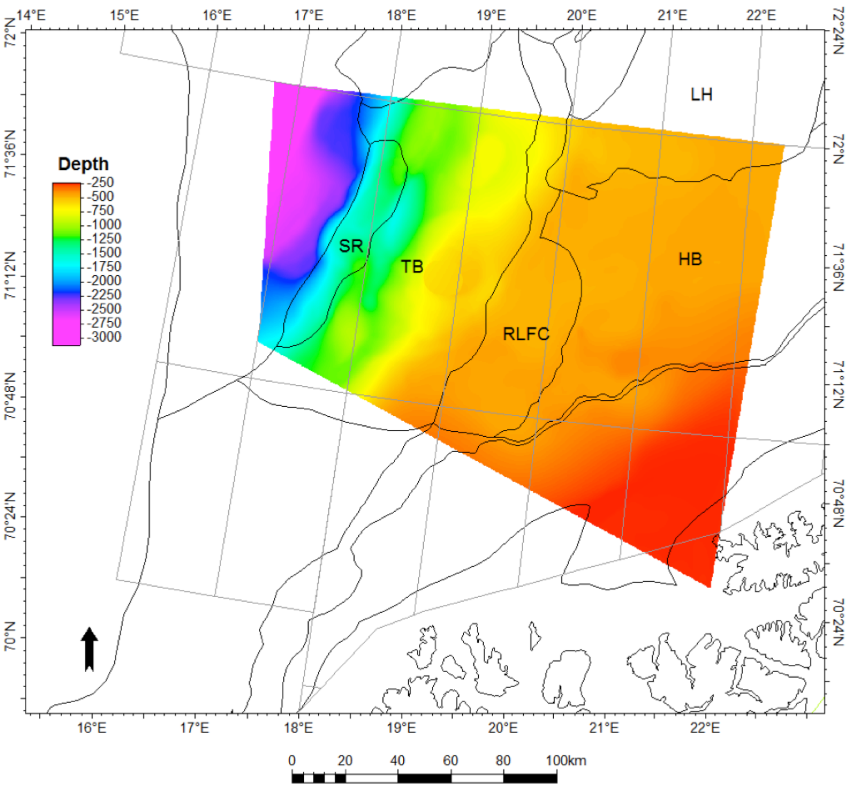

Figure 6. Depth map Intra Late Eocene.

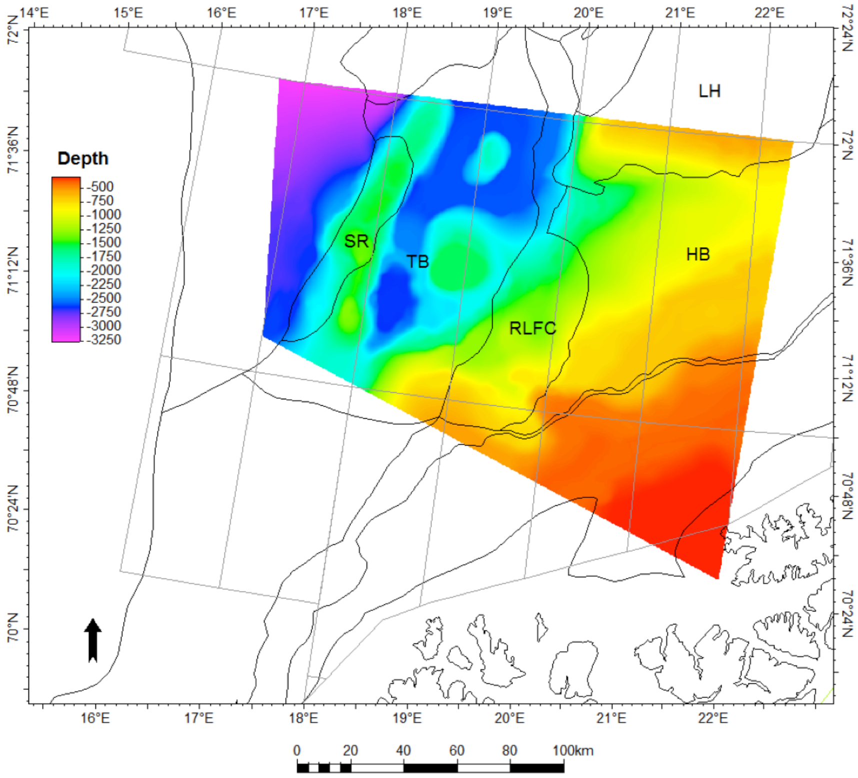

Figure 7. Depth map Base Torsk.

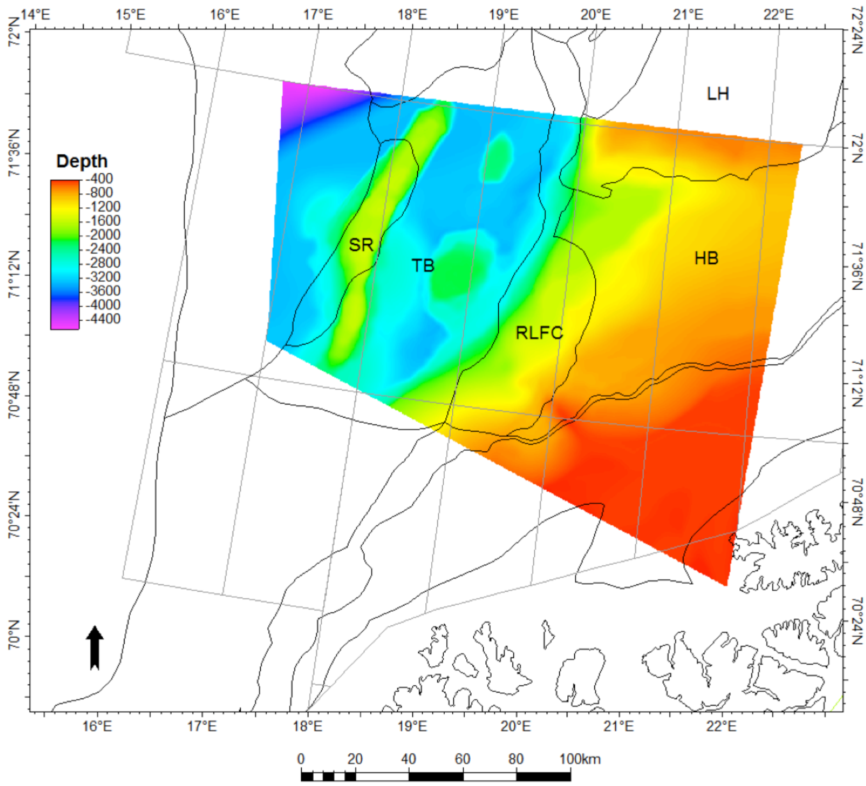

Figure 8. Depth map Top Kolmule.

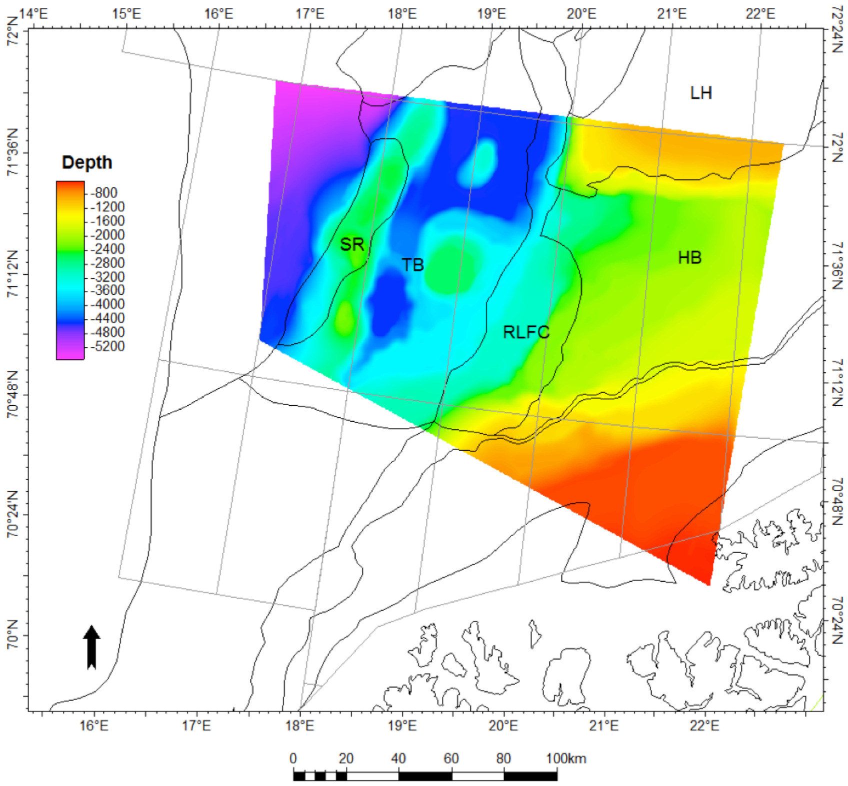

Figure 9. Depth map Top Hekkingen.

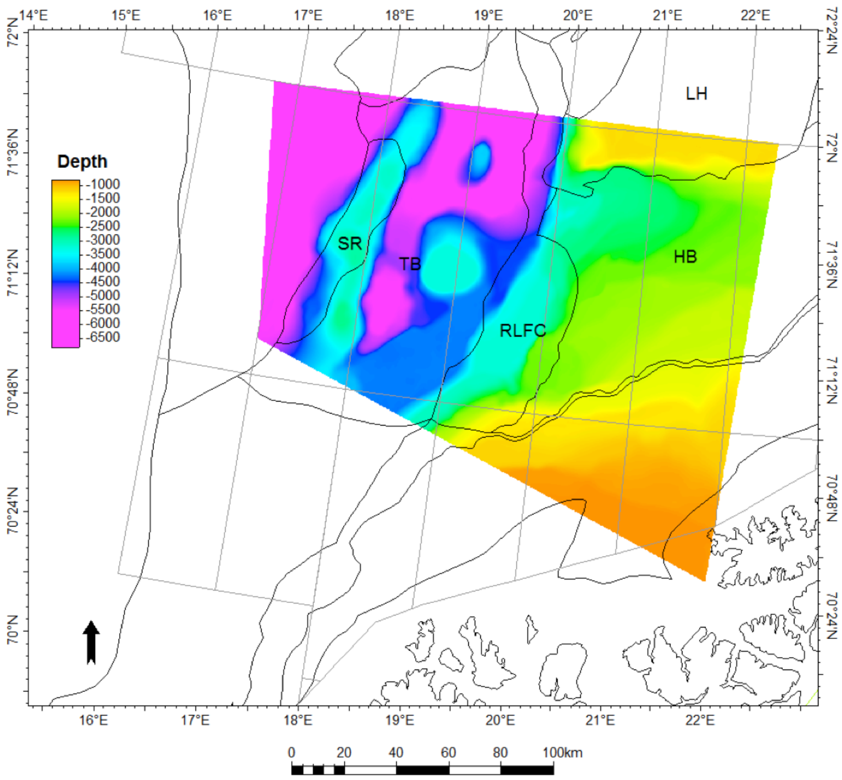

Figure 10. Depth map Base Hekkingen.